Correspondence

OFDM-Aided Differential Space–Time Shift Keying Using Iterative Soft Multiple-Symbol Differential Sphere Decoding

Mohammad Ismat Kadir, Sheng Chen, K. V. S. Hari, K. Giridhar, and Lajos Hanzo

***Abstract*—Soft-decision multiple-symbol differential sphere decoding (MSDSD) is proposed for orthogonal frequency-division multiplexing (OFDM)-aided differential space–time shift keying (DSTSK)-aided transmission over frequency-selective channels. Specifically, the DSTSK signaling blocks are generated by the channel-encoded source information and the space–time (ST) blocks are appropriately mapped to a number of OFDM subcarriers. After OFDM demodulation, the DSTSK signal is noncoherently detected by our soft-decision MSDSD detector. A novel soft-decision MSDSD detector is designed, and the associated decision rule is derived for the DSTSK scheme. Our simulation results demonstrate that an SNR reduction of 2 dB is achieved by the proposed scheme using an MSDSD window size of $N_w = 4$ over the conventional soft-decision-aided differential detection benchmarker, while communicating over dispersive channels and dispensing with channel estimation (CE).**

***Index Terms*—Extrinsic information transfer (EXIT) chart, iterative decoding, multiple-symbol differential sphere decoding (MSDSD), orthogonal frequency-division multiplexing (OFDM), space–time shift keying (STSK).**

I. Introduction

Space–time shift keying (STSK) [1]–[3] has emerged as a beneficial multiple-input–multiple-output (MIMO) concept. STSK bridges the gap between the flexible diversity–multiplexing tradeoff provided by linear dispersion codes (LDCs) [4], [5] and the low-complexity design of spatial modulation (SM) [6]. Similar to the LDCs, STSK spreads the user information to both the spatial and time dimensions, but instead of simultaneously activating all the dispersion matrices (DMs), it transmits an additional $\log_2 Q$ bits by activating one out of Q DMs. To overcome the performance degradation of the STSK scheme in wideband channels, orthogonal frequency-division multiplexing (OFDM)-aided STSK [7] and orthogonal frequency-division multiple-access /single-carrier frequency-division multiple-access-aided STSK [8] have also been proposed. The previous STSK studies [1], [2] demonstrate that coherent STSK performs well in conjunction with perfect channel state information (CSI) but exhibits a severe error floor in the presence of channel estimation (CE) errors.

Manuscript received July 27, 2013; revised December 21, 2013; accepted February 8, 2014. This work was supported in part by the Research Council U.K. under the auspices of the India–U.K. Advanced Technology Center of the European Union under the Concerto Project and in part by the European Research Council under its Advanced Fellow Grant. The review of this paper was coordinated by Prof. Y. Su.

M. I. Kadir, S. Chen, and L. Hanzo are with the School of Electronics and Computer Science, University of Southampton, Southampton SO17 1BJ, U.K. (e-mail: mik1g09@ecs.soton.ac.uk; sqc@ecs.soton.ac.uk; lh@ecs.soton.ac.uk).

K. V. S. Hari is with the Department of Electrical Communication Engineering, Indian Institute of Science, Bangalore 560012, India (e-mail: hari@ece.iisc.ernet.in).

K. Giridhar is with the Department of Electrical Engineering, Indian Institute of Technology Madras, Chennai 600036, India (e-mail: giri@tenet.res.in).

Color versions of one or more of the figures in this paper are available online at http://ieeexplore.ieee.org.

Digital Object Identifier 10.1109/TVT.2014.2306654

Differential STSK (DSTSK) employing conventional differential detection (CDD) has also been proposed for the sake of dispensing with the CE [2] and thus to eliminate the potentially high-Doppler-dependent pilot overhead. However, CDD suffers from a typical 3-dB performance penalty in low-Doppler scenarios. Furthermore, an irreducible error floor may be observed in a high-mobility scenario characterized by a high Doppler frequency. To circumvent the performance degradation of CDD, multiple-symbol differential detection (MSDD) was proposed for differential phase-shift keying (DPSK) in [9]. MSDD uses the fading-plus-noise statistics of the channel for jointly detecting $(N_w - 1)$ information symbols from N_w number of consecutively received symbols, where N_w is usually referred to as the *observation window size*. The performance improvement of MSDD is, however, achieved at the cost of increased complexity, which increases exponentially with N_w. For mitigating this potentially excessive complexity, sphere decoding (SD) was invoked for MSDD in the context of multiple-symbol differential sphere decoding (MSDSD) in [10] and [11]. Hard-decision MSDSD was conceived in [12] for a DSTSK scheme operating in nondispersive channels. As a further advance, inspired by the near-capacity performance of turbo detection [13], [14], a soft-decision MSDSD scheme was also designed for DPSK in [15]. Furthermore, the concept of differential space–frequency modulation employing MSDSD in conjunction with a specific subcarrier allocation was proposed in [16] for exploiting both the achievable spatial- and frequency-domain diversity. However, the conception of the soft-decision-MSDSD-aided DSTSK designed for realistic dispersive scenarios constitutes an unexplored open problem.

Against this background, we conceive a novel soft-decision MSDSD for OFDM-based DSTSK operating in frequency-selective channels. The main contributions of this paper are as follows.

1) A novel soft-decision-aided MSDSD is proposed for OFDM-aided DSTSK operating in dispersive channels. The decision rule of the soft-decision MSDSD is deduced by considering the construction of DSTSK codewords based on the DMs, the Doppler frequency, the OFDM system parameters, and the generation of soft information.
2) A lower bound of the detection complexity is deduced, which is verified by simulations.

The remainder of this paper is organized as follows. In Section II, an overview of the proposed channel-coded OFDM-aided DSTSK scheme is provided. The soft-decision MSDSD is modeled in Section III. In Section IV, both the complexity imposed by the system is quantified. The performance of the soft-decision MSDSD-aided DSTSK scheme is investigated in Section V. Finally, we conclude in Section VI.

Notations: We use capital boldface letters to denote matrices, whereas $\{\cdot\}^T$, $\{\cdot\}^H$, $\mathrm{tr}(\cdot)$, $\det[\cdot]$, and $\|\cdot\|$ are used to represent the transpose, the Hermitian transpose, the trace, the determinant, and the Euclidean norm of the matrix "$\cdot$," respectively. The notations $\mathcal{E}\{\cdot\}$, $\cdot^*$, and $P(\cdot)$ are used to denote the expected value, the complex conjugate, and the probability of "$\cdot$" respectively, whereas $\otimes$ and $\boldsymbol{I}_T$ represent the Kronecker product and the $(T \times T)$ identity matrix, respectively. A symmetric $(N_w \times N_w)$ Toeplitz matrix is denoted $\mathrm{toeplitz}\{x_1, \ldots, x_{N_w}\}$, whereas $\mathrm{diag}\{\boldsymbol{X}_1, \ldots, \boldsymbol{X}_{N_w}\}$ indicates a block-diagonal matrix with the matrices $\boldsymbol{X}_1, \ldots, \boldsymbol{X}_{N_w}$ on its main diagonal. Furthermore, $\mathcal{CN}(\mu, \sigma^2)$ refers to the circularly symmetric complex Gaussian distribution with mean μ and variance σ^2.

0018-9545 © 2014 IEEE. Personal use is permitted, but republication/redistribution requires IEEE permission.
See http://www.ieee.org/publications_standards/publications/rights/index.html for more information.

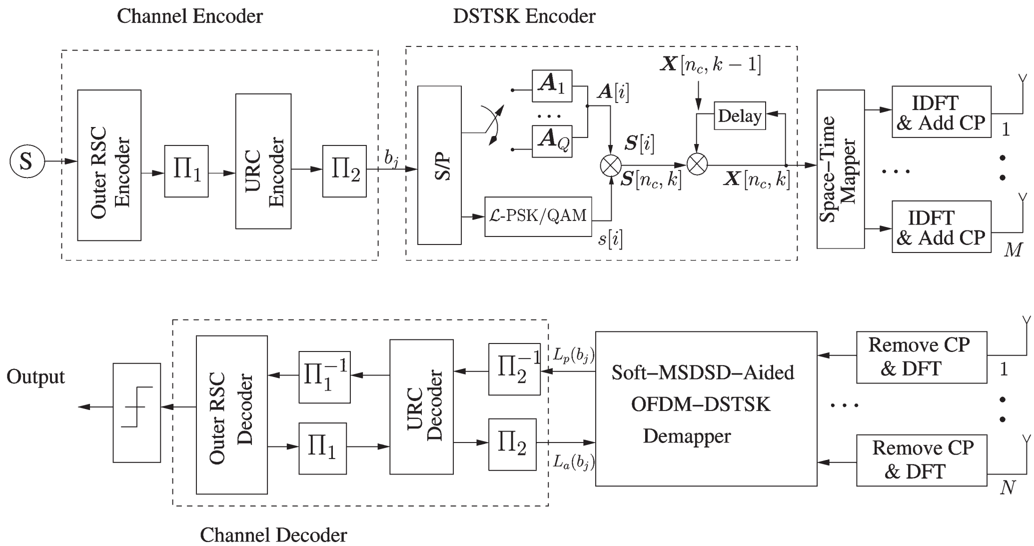

Fig. 1. Transceiver architecture of the proposed concatenated channel-coding-aided DSTSK scheme relying on the soft-decision MSDSD as the inner decoder.

II. System Model

We consider a channel-coded OFDM-aided DSTSK transceiver employing M transmit and N receive antenna elements (AEs), as shown in Fig. 1. The channel encoder/decoder blocks of Fig. 1 may incorporate a general channel coding scheme that supports soft-decision decoding at affordable complexity. A pragmatic coding architecture might be an appropriately interleaved serially concatenated recursive convolutional code (RSC) and unity rate code (URC)-aided scheme [17]–[19], as shown in Fig. 1.

The source bits are first channel encoded by the RSC code, and the encoded bits are then interleaved by a random bit interleaver Π_1. Following URC precoding, the interleaved bits are further interleaved by a second interleaver Π_2. The resultant bits are then mapped to STSK codewords, which are further mapped to N_c parallel subcarriers and then differentially encoded in the time domain (TD), i.e., across the consecutive OFDM symbols of the same subcarrier. The DSTSK codewords are then OFDM modulated, while incorporating appropriate cyclic prefixes (CPs).

The signal received is first OFDM demodulated and then input to the DSTSK soft-decision MSDSD demapper. The extrinsic soft information is then iteratively exchanged between the three soft-in–soft-out components, namely, the DSTSK demapper, the URC decoder, and the RSC decoder, before finally outputting the estimated bits [8], [19].

A. DSTSK Architecture and OFDM Layout

The STSK encoder generates space–time (ST) codewords from the source information by activating a single DM in any symbol duration in conjunction with the classic modulated symbols for transmission over T time slots using M transmit AEs [1], [2]. More specifically, each STSK signaling block $\boldsymbol{S}[i] \in \mathbb{C}^{T\times M}$ is created from $\log_2(\mathcal{L}\cdot Q)$ source bits according to [1], [2]

$$\boldsymbol{S}[i] = s[i]\boldsymbol{A}[i] \tag{1}$$

where $s[i]$ is an $\mathcal{L}$-ary constellation symbol represented by $\log_2 \mathcal{L}$ bits, and $\boldsymbol{A}[i] \in \mathbb{C}^{T\times M}$ is the specific DM activated from the set of Q DMs $\boldsymbol{A}_q (q = 1,\ldots,Q)$, as determined by the remaining $\log_2 Q$ bits. The DMs $\boldsymbol{A}_q (q = 1,\ldots,Q)$ are unitary matrices generated by employing an exhaustive search for minimizing the objective function constituted by the pairwise error probability of the codewords [5], [12], [20], [21] under the power constraint in [2] expressed by $\mathrm{tr}(\boldsymbol{A}_q^H\boldsymbol{A}_q) = T\,\forall\, q$. The resultant STSK system is then uniquely and unambiguously described by the parameters $(M,\, N,\, T,\, Q,\, \mathcal{L})$.

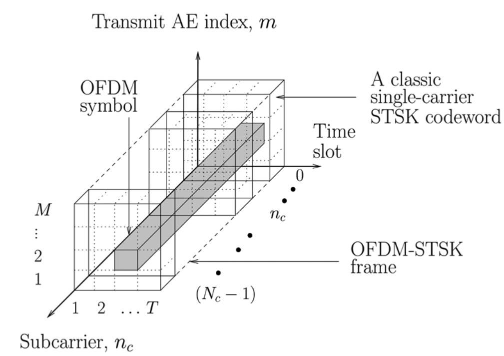

Fig. 2. Mapping of the STSK codewords to N_c parallel OFDM subcarriers showing the construction of an OFDM-STSK frame and OFDM symbols. After being appropriately mapped to the subcarriers, the codewords are differentially encoded in the TD and transmitted over dispersive channels by M transmit AEs over T time-slots.

We observe that the STSK codeword $\boldsymbol{S}[i]$ belongs to a set $\boldsymbol{\mathcal{S}}$ of $(\mathcal{L}\cdot Q)$ codeword matrices defined by

$$\boldsymbol{\mathcal{S}} \triangleq \{s_l \boldsymbol{A}_q | \,(q \in \{1,\ldots,Q\}, \quad l \in \{1,\ldots,\mathcal{L}\})\}. \tag{2}$$

The STSK codewords are mapped to N_c parallel subcarriers, as shown in Fig. 2, before being differentially encoded. As shown in Fig. 2, N_c consecutive STSK codewords are arranged in parallel to form an OFDM-STSK frame, and OFDM modulation is carried out over each shaded symbol pipe, which constitutes an OFDM symbol. We may represent the codeword $\boldsymbol{S}[i]$ by $\boldsymbol{S}[n_c,\, k]$, so that the overall codeword index i is related to the OFDM frame index k and the subcarrier index n_c by $i = kN_c + n_c$, $n_c = 0, 1, \ldots, (N_c - 1)$. Additionally, we invoke differential encoding in the TD, i.e., differential encoding is performed across the consecutive OFDM symbols of the same subcarrier. We have chosen TD differential encoding/decoding because we have conceived our scheme for continuous transmissions, as opposed to the FD differential encoding/decoding across adjacent FD subcarriers, which is more suitable for burst transmissions. To facilitate convenient differential encoding, we assume $M = T$. Furthermore, directly generated unitary DMs are used in the proposed scheme for avoiding the nonlinear Cayley transform [2], [12]. The codewords

$\boldsymbol{S}[n_c, k]$ are thus differentially encoded to form the transmit blocks $\boldsymbol{X}[n_c, k]$ $(k = 0, 1, 2, \ldots)$ according to [16]

$$\boldsymbol{X}[n_c, k] = \begin{cases} \boldsymbol{X}[n_c, k-1]\boldsymbol{S}[n_c, k], & k = 1, 2, \ldots \\ \boldsymbol{I}_T & k = 0. \end{cases} \tag{3}$$

The DSTSK codewords are then transmitted after the N_c-point inverse discrete Fourier transform (DFT) operation and appropriate CP incorporation.

B. Channel Model

Each link between the mth transmit and nth receive AE is assumed a frequency-selective channel, but as a benefit of OFDM-based transmission, each dispersive channel is then partitioned into N_c low-rate parallel frequency-flat subchannels [22]. The complex-valued fading gain $h_{m,n}[n_c, k]$ $(m = 1, 2, \ldots, M;\ n = 1, 2, \ldots, N)$ obeys the distribution $\mathcal{CN}(0, 1)$ associated with an autocorrelation function based on Clarke's model [23]: $\varphi_{hh}[n_c, \kappa] \triangleq \mathcal{E}\{h_{m,n}[n_c, k] h^*_{m,n}[n_c, k+\kappa]\} = J_0(2\pi\kappa f_d)$, where J_0 denotes the zeroth-order Bessel function of the first kind, and $f_d = f_m \mathcal{T}$ is the normalized maximum Doppler frequency, whereas f_m and $1/\mathcal{T}$ represent the maximum Doppler frequency and the symbol rate, respectively. The fading is assumed quasi-static, i.e., the channel's complex-valued envelope remains approximately constant during the transmission of an OFDM STSK frame.

Given the aforementioned assumptions, the received signal $\boldsymbol{Y}[n_c, k] \in \mathbb{C}^{T\times N}$ obtained after CP removal and DFT may be expressed by [16], [22]

$$\boldsymbol{Y}[n_c, k] = \boldsymbol{X}[n_c, k]\boldsymbol{H}[n_c, k] + \boldsymbol{V}[n_c, k] \tag{4}$$

where $\boldsymbol{X}[n_c, k] \in \mathbb{C}^{T\times M}$ represents the codeword transmitted and $\boldsymbol{H}[n_c, k] \in \mathbb{C}^{M\times N}$ denotes the FD channel transfer matrix, with its (m, n)th entry given by $h_{m,n}[n_c, k]$. Furthermore, $\boldsymbol{V}[n_c, k] \in \mathbb{C}^{T\times N}$ is the additive white Gaussian noise (AWGN) with entries of $v_{T_i, n}[n_c, k] \sim \mathcal{CN}(0, \sigma_n^2)$.

III. MSDSD Receiver

This section introduces the maximum-likelihood MSDSD (ML-MSDSD), the maximum *a posteriori* MSDSD (MAP-MSDSD) algorithm, and the generation of the log-likelihood ratios (LLRs) for the soft-decision-MSDSD-aided OFDM DSTSK.

A. ML-MSDSD for OFDM-Aided DSTSK

The ML-MSDD processes N_w consecutively received space–time blocks corresponding to the n_cth subcarrier given by $\bar{\boldsymbol{Y}}[n_c, k] \triangleq [\boldsymbol{Y}^T[n_c, k-N_w+1], \ldots, \boldsymbol{Y}^T[n_c, k]]^T$ and finds the ML estimates $\hat{\bar{\boldsymbol{X}}}[n_c, k]$ of the corresponding N_w transmitted blocks $\bar{\boldsymbol{X}}[n_c, k] \triangleq [\boldsymbol{X}^T[n_c, k-N_w+1], \ldots, \boldsymbol{X}^T[n_c, k]]^T$ [24]. Since the differentially encoded blocks $\boldsymbol{X}[n_c, k]$ are related to the STSK codewords by the one-to-one relationship expressed by (3), the ML-MSDD in turn estimates $(N_w - 1)$ STSK codewords given by $\bar{\boldsymbol{S}}[n_c, k] \triangleq [\boldsymbol{S}^T[n_c, k-N_w+2], \ldots, \boldsymbol{S}^T[n_c, k]]^T$, which further estimates the source bits mapped to the STSK codewords.

Defining a block-diagonal matrix $\bar{\boldsymbol{X}}_D[n_c, k]$ by $\bar{\boldsymbol{X}}_D[n_c, k] \triangleq \text{diag}\{\boldsymbol{X}[n_c, k-N_w+1], \ldots, \boldsymbol{X}[n_c, k]\}$, $\bar{\boldsymbol{H}}[n_c, k] \triangleq [\boldsymbol{H}^T[n_c, k-N_w+1], \ldots, \boldsymbol{H}^T[n_c, k]]^T$, and $\bar{\boldsymbol{V}}[n_c, k] \triangleq [\boldsymbol{V}^T[n_c, k-N_w+1], \ldots, \boldsymbol{V}^T[n_c, k]]^T$, the N_w-block received sequence can be expressed by [11], [24]

$$\bar{\boldsymbol{Y}}[n_c, k] = \bar{\boldsymbol{X}}_D[n_c, k]\bar{\boldsymbol{H}}[n_c, k] + \bar{\boldsymbol{V}}[n_c, k] \tag{5}$$

where

$$\bar{\boldsymbol{Y}}[n_c, k] \in \mathbb{C}^{N_w M\times N} \quad \bar{\boldsymbol{V}}[n_c, k] \in \mathbb{C}^{N_w M\times N}$$
$$\bar{\boldsymbol{H}}[n_c, k] \in \mathbb{C}^{N_w M\times N} \quad \bar{\boldsymbol{X}}_D[n_c, k] \in \mathbb{C}^{N_w M\times N_w M}.$$

For the sake of notational simplicity, we omit the subcarrier index and time index $[n_c, k]$ in the following and refer to the μth submatrix of a block matrix, e.g., $\boldsymbol{B}$ by the subscripted matrix $\boldsymbol{B}_\mu$. Under the assumption that $h_{m,n}$ and $v_{T_i,n}$ $(m = T_i = 1, 2, \ldots, M, n = 1, 2, \ldots, N)$ are zero-mean Gaussian random processes, the probability density function of $\bar{\boldsymbol{Y}}$ conditioned on $\bar{\boldsymbol{X}}_D$ is given by [25], [26]

$$P(\bar{\boldsymbol{Y}}|\bar{\boldsymbol{X}}_D) = \frac{1}{(\pi^{N_w M}\det[\boldsymbol{\Lambda}_Y])^N} \exp\left\{-\text{tr}\left(\bar{\boldsymbol{Y}}^H \boldsymbol{\Lambda}_Y^{-1}\bar{\boldsymbol{Y}}\right)\right\} \tag{6}$$

where $\boldsymbol{\Lambda}_Y$ is defined by $\boldsymbol{\Lambda}_Y \triangleq \mathcal{E}\{\bar{\boldsymbol{Y}}\bar{\boldsymbol{Y}}^H|\bar{\boldsymbol{X}}_D\}$. The ML estimate $\hat{\bar{\boldsymbol{X}}}$ under the assumption of quasi-static fading and unitary $\bar{\boldsymbol{X}}_D$ reduces to [26], [27]

$$\hat{\bar{\boldsymbol{X}}} = \arg\max_{\tilde{\bar{\boldsymbol{X}}}} P(\bar{\boldsymbol{Y}}|\bar{\boldsymbol{X}}_D) = \arg\min_{\tilde{\bar{\boldsymbol{X}}}} \left\{\text{tr}\left(\bar{\boldsymbol{Y}}^H\boldsymbol{\Lambda}_Y^{-1}\bar{\boldsymbol{Y}}\right)\right\}. \tag{7}$$

Here, the conditional covariance matrix $\boldsymbol{\Lambda}_Y$ is related to the channel parameters [25], [26] by

$$\boldsymbol{\Lambda}_Y^{-1} = \frac{1}{N}\bar{\boldsymbol{X}}_D(\boldsymbol{\Lambda}^{-1}\otimes \boldsymbol{I}_M)\bar{\boldsymbol{X}}_D^H \tag{8}$$

where we have $\boldsymbol{\Lambda} \triangleq (\boldsymbol{\psi}_{hh} + \sigma_n^2\boldsymbol{I}_{N_w})$ and $\boldsymbol{\psi}_{hh} \triangleq \texttt{toeplitz}\{\varphi_{hh}[n_c, 0], \ldots, \varphi_{hh}[n_c, (N_w-1)]\}$, with the component autocorrelation functions $\varphi_{hh}[n_c, \kappa]$ being identical for all spatial channels. Applying the Cholesky factorization of $\boldsymbol{\Lambda}^{-1} = \boldsymbol{U}^H\boldsymbol{U}$ with the upper triangular matrix $\boldsymbol{U}$ and considering the identity $\text{tr}(\boldsymbol{\mathcal{X}}\boldsymbol{\mathcal{X}}^H) = \|\boldsymbol{\mathcal{X}}\|^2$ for any matrix $\boldsymbol{\mathcal{X}}$, the ML-MSDD decision rule can be deduced from (6), yielding [11]

$$\hat{\bar{\boldsymbol{X}}} = \arg\min_{\tilde{\bar{\boldsymbol{X}}}} \left\{\sum_{\mu=1}^{N_w}\left\|\boldsymbol{Y}^H_{\mu,\mu}\tilde{\boldsymbol{X}}_\mu + \sum_{\nu=\mu+1}^{N_w}\left(\boldsymbol{Y}^H_{\mu,\nu}\tilde{\boldsymbol{X}}_\nu\right)\right\|^2\right\} \tag{9}$$

where $\boldsymbol{Y}^H_{\mu,\nu}$ is defined by $\boldsymbol{Y}^H_{\mu,\nu} \triangleq \boldsymbol{Y}_\nu u_{\mu,\nu}$, and $u_{\mu,\nu}$ represents the (μ, ν)th element of $\boldsymbol{U}$. Still referring to (9), $\hat{\bar{\boldsymbol{X}}}$ denotes the *estimate* of $\bar{\boldsymbol{X}}_D$, whereas $\tilde{\boldsymbol{X}}_\mu$ refers to the μth *candidate* submatrix of $\bar{\boldsymbol{X}}_D$.

Since the ML metric of (9) is invariant to a phase shift common to all elements of $\tilde{\boldsymbol{X}}_\mu\ \forall\mu$ corresponding to the same $\bar{\boldsymbol{S}}$ (where $\boldsymbol{S}_\lambda^T \in \boldsymbol{\mathcal{S}}\ \forall\lambda$), the accumulated differential matrices may be expressed as [15]

$$\boldsymbol{\mathcal{A}}_\nu = \begin{cases} \prod_{\lambda=\nu}^{N_w-1}\boldsymbol{S}^H_\lambda, & 1 \leqslant \nu \leqslant (N_w-1) \\ \boldsymbol{I}_T, & \nu = N_w. \end{cases} \tag{10}$$

For the sake of reducing the complexity associated with an exhaustive search, we employ MSDSD similar to [10] and [11] to search through the candidate set lying within a sphere of radius ρ_s as follows:

$$\sum_{\mu=1}^{N_w}\left\|\boldsymbol{Y}^H_{\mu,\mu}\boldsymbol{A}_\mu + \sum_{\nu=\mu+1}^{N_w}\left(\boldsymbol{Y}^H_{\mu,\nu}\boldsymbol{\mathcal{A}}_\nu\right)\right\|^2 \le \rho_s^2. \tag{11}$$

B. MAP-MSDSD

Assuming the STSK codewords to be mutually independent, (6) and (9) yield [15]:

$$\begin{aligned} &-\ln\left(P(\bar{\boldsymbol{S}}|\bar{\boldsymbol{Y}})\right) \\ &\quad\propto -\ln\left(P(\bar{\boldsymbol{Y}}|\bar{\boldsymbol{S}})\right) - \ln\left(P(\bar{\boldsymbol{S}})\right) \\ &\quad\propto \sum_{\mu=1}^{N_w}\left\{\left\|\boldsymbol{Y}^H_{\mu,\mu}\boldsymbol{\mathcal{A}}_\mu + \sum_{\nu=\mu+1}^{N_w}\boldsymbol{Y}^H_{\mu,\nu}\boldsymbol{\mathcal{A}}_\nu\right\|^2 - \ln\left(P(\boldsymbol{S}_\mu)\right)\right\}. \end{aligned} \tag{12}$$

The MAP-MSDSD may be thus expressed as

$$\sum_{\mu=1}^{(N_w-1)}\left(\left\|\sum_{\nu=\mu}^{N_w}\left(\boldsymbol{Y}^H_{\mu,\,\nu}\boldsymbol{\mathcal{A}}_\nu\right)\right\|^2-\ln\left(P(\boldsymbol{S}_\mu)\right)\right)$$
$$\leq \rho_s^2-\|u_{N_w,N_w}\boldsymbol{Y}_{N_w}\|^2\triangleq\rho^2. \quad (13)$$

Clearly, the codeword $\boldsymbol{S}_\mu$ obeys the specific distance criterion [10], [12], [28] that the current partial Euclidean distance (PED) d_μ^2 is the sum of the previous PED $d_{\mu+1}^2$ and the distance increment $\triangle_\mu^2$, i.e.,

$$\begin{aligned} d_\mu^2 &\triangleq \triangle_\mu^2+d_{\mu+1}^2\\ &=\left\|u_{\mu,\mu}\boldsymbol{Y}_\mu\boldsymbol{\mathcal{A}}_{\mu+1}\boldsymbol{S}_\mu^H+\sum_{\nu=\mu+1}^{N_w}u_{\mu,\,\nu}\boldsymbol{Y}_\nu\boldsymbol{\mathcal{A}}_\nu\right\|^2-\ln\left(P(\boldsymbol{S}_\mu)\right)\\ &\quad+\sum_{\iota=\mu+1}^{(N_w-1)}\left(\left\|\sum_{\nu=\iota}^{N_w}u_{\iota,\nu}\boldsymbol{Y}_\nu\boldsymbol{\mathcal{A}}_\nu\right\|^2-\ln\left(P(\boldsymbol{S}_\iota)\right)\right)\leq\rho^2. \quad (14)\end{aligned}$$

Similar to the MSDSD principle described in [10] and [15], the MAP-MSDSD is initialized with $\mu=(N_w-1)$ and then proceeds by applying the search criterion of (14) until $\mu=1$, where the search radius is updated to $\rho^2=d_1^2$, and the search is repeated by commencing from $\mu=2$ until $\mu=(N_w-1)$ is reached. If the new search does not provide a better estimate, the previous estimate is retained.

C. Log-Likelihood Ratio and Soft-Decision-MSDSD-Aided OFDM DSTSK

The soft demapper relies on the *a priori* information gleaned from the URC decoder and the MAP-MSDSD. A high interleaver depth is assumed so that the permuted bits may be treated as being independent. The LLR corresponding to the bit b_j interleaved by the interleaver Π_2 of Fig. 1 is defined by [29] $L_a(b_j)\triangleq\ln(P(b_j=b)/P(b_j=\bar{b}))$, where $b\in\{0,1\}$, and the jth bit $b_j=b$ corresponds to the MAP-MSDSD estimate $\hat{\hat{\boldsymbol{S}}}$, whereas $\bar{b}$ indicates its complement. The *a posteriori* LLR $L_p(\cdot)$ of b_j may be then approximated by the maximum-logarithmic-MAP (max-log-MAP) algorithm [14], [15], i.e.,

$$\begin{aligned} &L_p(b_j)\\ &=\ln\frac{P(b_j=b|\boldsymbol{Y})}{P(b_j=\bar{b}|\boldsymbol{Y})}\\ &\approx\ln\frac{\max_{\hat{\boldsymbol{S}}:b_j=b}\left[-\sum_{\mu=1}^{N_w}\left\|\sum_{\nu=\mu}^{N_w}\left(\boldsymbol{Y}^H_{\mu,\,\nu}\hat{\boldsymbol{\mathcal{A}}}_\nu\right)\right\|^2+\ln\left(P(\hat{\hat{\boldsymbol{S}}})\right)\right]}{\max_{\hat{\boldsymbol{S}}:b_j=\bar{b}}\left[-\sum_{\mu=1}^{N_w}\left\|\sum_{\nu=\mu}^{N_w}\left(\boldsymbol{Y}^H_{\mu,\,\nu}\hat{\boldsymbol{\mathcal{A}}}_\nu\right)\right\|^2+\ln\left(P(\hat{\hat{\boldsymbol{S}}})\right)\right]}\\ &=-\sum_{\mu=1}^{N_w}\left\|\sum_{\nu=\mu}^{N_w}\left(\boldsymbol{Y}^H_{\mu,\,\nu}\hat{\boldsymbol{\mathcal{A}}}^b_\nu\right)\right\|^2+\ln\left(P(\hat{\hat{\boldsymbol{S}}}^b)\right)\\ &\quad+\sum_{\mu=1}^{N_w}\left\|\sum_{\nu=\mu}^{N_w}\left(\boldsymbol{Y}^H_{\mu,\,\nu}\hat{\boldsymbol{\mathcal{A}}}^{\bar{b}}_\nu\right)\right\|^2-\ln\left(P(\hat{\hat{\boldsymbol{S}}}^{\bar{b}})\right) \quad (15)\end{aligned}$$

where $\hat{\hat{\boldsymbol{S}}}^b$ and $\hat{\hat{\boldsymbol{S}}}^{\bar{b}}$ represent the MAP-MSDSD estimate and the constrained estimate associated with $b_j=\bar{b}$, respectively.

The extrinsic LLR $L_e(\cdot)$ for b_j is now evaluated by combining the *a posteriori* and *a priori* LLR: $L_e(b_j)=L_p(b_j)-L_a(b_j)$. The extrinsic information extracted from the soft-decision MSDSD demapper is iteratively exchanged with the URC decoder of Fig. 1, which forms the *inner* iteration, whereas the exchange of extrinsic information between the URC decoder and the RSC decoder of Fig. 1 may be termed as the *outer* iteration. Note that, for each outer iteration between the RSC decoder and the URC decoder, several inner iterations may be invoked between the URC and the soft-decision-MSDSD-aided DSTSK demapper [2], [19]. Finally, the RSC decoder generates *a posteriori* LLRs, from which the source bits are estimated.

IV. Complexity

Here, the complexity of the proposed scheme is detailed, and the complexity imposed by the MAP-MSDSD is quantified.

Equation (2) shows that there exists $(\mathcal{L}\cdot Q)$ legitimate codeword matrices for each $\log_2(\mathcal{L}\cdot Q)$ bits of source information. The exhaustive-search-based solution to (9) involves a search in a $(\mathcal{L}\cdot Q)^{(N_w-1)}$ element space of candidate matrices $\tilde{\boldsymbol{X}}$ corresponding to all possible choices of $\tilde{\boldsymbol{S}}$. The ML-MSDSD associated with chosen sphere radius ρ imposes average complexity, which is lower bounded by [11]

$$C\geq\frac{(\mathcal{L}\cdot Q)^{N_w\zeta-1}-(\mathcal{L}\cdot Q)}{(\mathcal{L}\cdot Q)-1} \quad (16)$$

where

$$\zeta\triangleq\frac{\sigma_n^2(1+\epsilon)}{2\left(1+\sigma_n^2\right)}\quad \rho^2=(1+\epsilon)NMN_w,\quad \epsilon>0. \quad (17)$$

To quantify the complexity of the MAP-MSDSD scheme, we consider the number of real-valued multiplication operations (RMOs) required for obtaining a single soft-output value, which is used as our complexity metric. The lower bound of the complexity may be obtained if the number of RMOs required for computing the soft outputs corresponding to the first codeword estimate $\hat{\hat{\boldsymbol{S}}}^b$ is counted and if a single constrained estimate $\hat{\hat{\boldsymbol{S}}}^{\bar{b}}$ is taken into account [15]. Considering the upper diagonal nature of the matrix $\boldsymbol{U}$, we observe that $\boldsymbol{Y}^H_{\mu,\,\nu}$ is defined only for $\nu\geq\mu$ in the context of (9), although each $\boldsymbol{Y}^H_{\mu,\,\nu}$ is an $(N\times T)$-element matrix, where $T=M$. The computation of the $\boldsymbol{Y}^H_{\mu,\,\nu}$ terms in (15) thus involves a total of $2MN[1+2+\cdots+N_w]=MNN_w(N_w+1)$ RMOs, assuming real-valued autocorrelation functions of $\varphi_{hh}[n_c,\,\kappa]$. To compute the *a posteriori* LLRs given by (15), the number of RMOs associated with the computation of each $\|\sum_{\nu=\mu}^{N_w}(\boldsymbol{Y}^H_{\mu,\,\nu}\hat{\boldsymbol{\mathcal{A}}}^b_\nu)\|^2$ is $4M^2N(N_w-\mu+1)+2$. The number of RMOs required for generating $\log_2(\mathcal{L}\cdot Q)$ soft outputs corresponding to a single codeword estimate $\hat{\hat{\boldsymbol{S}}}^b$ is thus given by

$$\begin{aligned}\text{RMO}[\hat{\hat{\boldsymbol{S}}}^b]&=MNN_w(N_w+1)+\sum_{\mu=1}^{N_w}\left[4M^2N(N_w-\mu+1)+2\right]\\ &=MN(2M+1)N_w(N_w+1)+2N_w. \quad (18)\end{aligned}$$

On the other hand, the number of RMOs related to each bit $\bar{b}$ of the constrained estimate $\hat{\hat{\boldsymbol{S}}}^{\bar{b}}$ is found to be $2N_w[M^2N(N_w+1)+1]$. The lower bound for the number of RMOs associated with the generation of a single soft output is thus $[MN(2M+1)/\log_2(\mathcal{L}\cdot Q)+2M^2N]N_w^2$ for large N_w. The complexity of the scheme, however, depends on a number of parameters, such as on the channel SNR, on the autocorrelation function of the channel's fading plus noise, and most importantly, on the *a priori* mutual information I_A of the inner decoder [15]. In Section V, the complexity of the MAP-MSDSD will be investigated as a function of the observation window width N_w parameterized by the available *a priori* information I_A.

TABLE I
ADOPTED VALUES OF MAIN SIMULATION PARAMETERS

Parameter	*Value*
Dispersive channel model	COST207-TU12
Fast fading envelope	Correlated Rayleigh fading
Normalized Doppler spread, f_d	0.01
Number of subcarriers, N_c	128
Length of cyclic prefix	32
Overall symbol duration	300 ns
STSK $(M, N, T, Q, \mathcal{L})$	(2, 2, 2, 4, 4)
RSC encoder and decoder	Half rate
	Constraint length=2
Generator polynomial	$(011, 010)_2$
Length of interleavers	200,000 bits
Outer iterations	11
Inner iterations	2

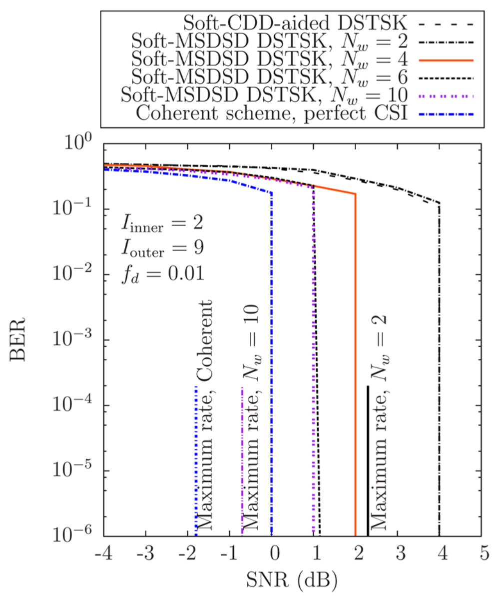

Fig. 3. Simulated BER performance of the soft-decision-MSDSD-aided OFDM DSTSK (2, 2, 2, 4, 4) scheme for transmission over dispersive COST207-TU12 channel with normalized Doppler frequency $f_d = 0.01$ and different observation window size $N_w = 2, 4, 6, 10$. The BER falls sharply after $I_{\text{outer}} = 9$ outer iterations as a benefit of employing the URC and the performance approaches that of the coherent scheme with perfect CSI with an increasing value of N_w.

V. PERFORMANCE RESULTS

Here, the performance of the proposed scheme is investigated using the parameters listed in Table I. We have employed the COST207-TU12 channel model for the links between each transmit–receive antenna pair. The power delay profile characterizing the 12 taps of the COST207-TU12 channel is detailed in [30] and [31]. As mentioned in Table I, we employ an RSC (2, 1, 2) outer code having octally represented generator polynomials of $(g_r, g) = (3, 2)_8$ as well as two random interleavers with a length of 200 000 bits.

Fig. 3 characterizes the achievable bit error rate (BER) of the proposed soft-decision-MSDSD-aided OFDM DSTSK scheme associated with observation window sizes of $N_w = 2, 4, 6, 10$ and compares to that achievable by the corresponding coherent scheme relying on perfect CSI. We observe that the proposed scheme has the benefit of dispensing with CE due to differential encoding, while mitigating the performance erosion of classic STSK by employing OFDM. Furthermore, the multiple-symbol detection partially mitigates the inherent performance penalty imposed by noncoherent detection. We observe in Fig. 3 that, as N_w increases, the BER performance gradually approaches that of the perfect CSI-oriented coherent scheme. Note that all the performance characteristics exhibit a vanishingly low BER after $I_{\text{outer}} = 9$ outer iterations, which is the explicit benefit of using the URC in the system. The URC is a low-complexity code, which has an infinite impulse response and hence assists the inner decoder in efficiently spreading the soft information [2], [19]. As a result, the extrinsic information transfer (EXIT) charts of Figs. 4 and 5 converge to the (1.0, 1.0) point of perfect decoding convergence, leading to a vanishingly low BER, thus eliminating the system's error floor. The maximum achievable rates for the corresponding scheme, where the scheme still exhibits an infinitesimally low BER were computed by exploiting the area property of EXIT charts [18], [32], [33] and are shown in Fig. 3 as the ultimate benchmark of the scheme.

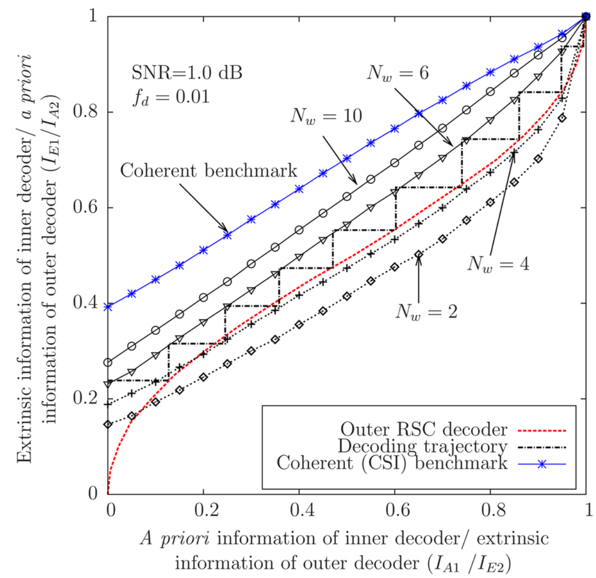

Fig. 4. EXIT charts of the inner decoders of the soft-decision-MSDSD-aided OFDM DSTSK (2, 2, 2, 4, 4) scheme at SNR = 1 dB with normalized Doppler frequency $f_d = 0.01$ and different observation window sizes $N_w = 2, 4, 6, 10$ and of the corresponding coherent system having perfect CSI at the receiver. At this SNR, we observe the inner EXIT charts with $N_w = 6, 10$ have an open EXIT tunnel and converge to the (1.0, 1.0) point of perfect convergence, indicating a sharp fall in the BER curve after $I_{\text{outer}} = 9$ outer iterations, which is confirmed by the decoding trajectory for $N_w = 6$. The EXIT charts with $N_w = 2, 4$ are, however, "pinched off"; thus, the BER at this SNR do not converge.

To elaborate further, Figs. 4 and 5 portray the EXIT charts of our proposed scheme at SNR = 1 and 4 dB, respectively. We observe in Fig. 4 that the inner decoder's EXIT charts recorded at SNR = 1 dB for $N_w = 2, 4$ are "pinched off," i.e., there remains no "open" EXIT tunnel, indicating a high residual BER. By contrast, the BER associated with $N_w = 6, 10$ may be expected to decrease sharply at this SNR after $I_{\text{outer}} = 9$ outer iterations, which is confirmed by the staircase-shaped Monte Carlo-simulation-based decoding trajectory [8], [13]. Fig. 5, on the other hand, shows the EXIT charts at SNR = 4 dB, where all the curves associated with $N_w = 2, 4, 6, 10$ exhibit an open EXIT tunnel, implying an infinitesimally low BER after $I_{\text{outer}} = 9$ iterations. The EXIT charts of the soft-decision-MSDSD-aided OFDM DSTSK recorded both for SNR = 1 dB and SNR = 4 dB are further compared in Figs. 4 and 5 to the ultimate benchmark of the coherent detector assuming perfect CSI at the receiver.

Fig. 6 characterizes the complexity associated with the MAP-MSDSD of the OFDM-aided DSTSK (2, 2, 2, 4, 4) scheme at SNR = 4 dB as a function of the window size N_w, parameterized by the

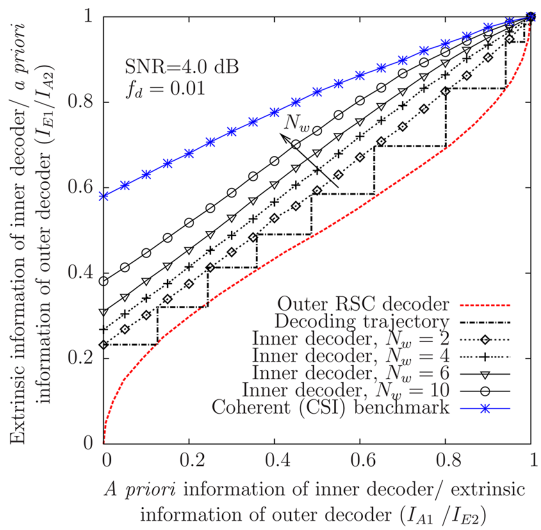

Fig. 5. EXIT charts of the inner decoders of the soft-decision-MSDSD-aided OFDM DSTSK (2, 2, 2, 4, 4) scheme at SNR $= 4$ dB with normalized Doppler frequency $f_d = 0.01$ and different observation window sizes $N_w = 2, 4, 6, 10$ and that of the corresponding coherent inner decoder as a benchmark. All the EXIT charts have a quite open EXIT tunnel at this SNR and converge to the (1.0, 1.0) point as a benefit of employing the URC, indicating a sharp fall in the BER curve after $I_{\text{outer}} = 9$ outer iterations, which is confirmed by the decoding trajectory.

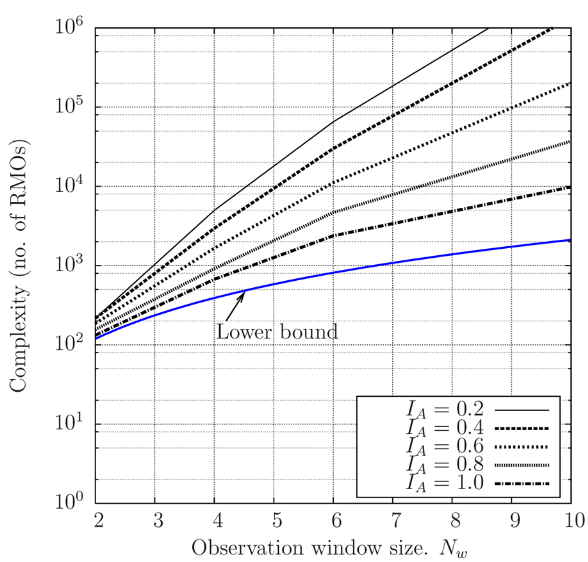

Fig. 6. Complexity in terms of the numbers of RMOs for the proposed DSTSK (2, 2, 2, 4, 4) scheme at SNR $= 4$ dB using the parameters of Table I as a function of observation window size N_w parameterized against the *a priori* mutual information of the inner decoder I_A. The complexity shoots up with $N_w > 6$, although the rate of increase in complexity slows down with increased *a priori* information.

a priori information I_A provided by the outer decoder for the demapper of Fig. 1. The *a priori* information I_A is measured by the average mutual information [13] between the *a priori* LLR $L_a(b_j)$ and the *a posteriori* LLR $L_p(b_j)$ of Fig. 1. The influence of the *a priori* information I_A on the complexity may be beneficially exploited in the context of adaptive system design [15], where N_w may be adaptively selected depending on the quality of the soft input. To be specific, the value of I_A increases during the consecutive decoding iterations, and we can flexibly increase N_w when the value of I_A is higher. The theoretical lower bound of the complexity quantified by the number of RMOs in Section IV is also shown as a benchmarker in Fig. 6. As expected, the complexity rapidly escalates upon increasing N_w, albeit it does not become excessively high, provided that the *a priori* information gleaned from the outer decoder is in the range of $I_A \geq 0.8$.

VI. Conclusion

We have proposed a soft-decision-MSDSD-aided multicarrier DSTSK scheme for communications over wideband channels. The OFDM-aided DSTSK provides a flexible diversity versus multiplexing gain tradeoff by spreading the source information across both the spatial and time dimensions, while mitigating the potential performance degradation imposed by the frequency selectivity of the channel. The turbo-principle-based soft-decision MSDSD facilitates joint decisions over a number of DSTSK codewords, while exploiting the fading-plus-noise statistics of the channel. We have demonstrated that the proposed soft-decision-MSDSD-aided DSTSK scheme provides substantial flexibility at moderate complexity owing to dispensing with CE. Furthermore, the MSDSD mitigates the performance degradation inflicted by the CDD scheme without an undue increase in computational complexity.

References

[1] S. Sugiura, S. Chen, and L. Hanzo, "A universal space–time architecture for multiple-antenna aided systems," *IEEE Commun. Surveys Tuts.*, vol. 14, no. 2, pp. 401–420, Second Quarter, 2012.

[2] S. Sugiura, S. Chen, and L. Hanzo, "Coherent and differential space–time shift keying: A dispersion matrix approach," *IEEE Trans. Commun.*, vol. 58, no. 11, pp. 3219–3230, Nov. 2010.

[3] S. Sugiura, S. Chen, and L. Hanzo, "Generalized space–time shift keying designed for flexible diversity-, multiplexing- and complexity-tradeoffs," *IEEE Trans. Wireless Commun.*, vol. 10, no. 4, pp. 1144–1153, Apr. 2011.

[4] B. Hassibi and B. M. Hochwald, "High-rate codes that are linear in space and time," *IEEE Trans. Inf. Theory*, vol. 48, no. 7, pp. 1804–1824, Jul. 2002.

[5] R. W. Heath, Jr. and A. Paulraj, "Linear dispersion codes for MIMO systems based on frame theory," *IEEE Trans. Signal Process.*, vol. 50, no. 10, pp. 2429–2441, Oct. 2002.

[6] R. Mesleh, H. Haas, S. Sinanovic, C. W. Ahn, and S. Yun, "Spatial modulation," *IEEE Trans. Veh. Technol.*, vol. 57, no. 4, pp. 2228–2241, Jul. 2008.

[7] M. Driusso, F. Babich, M. I. Kadir, and L. Hanzo, "OFDM aided space–time shift keying for dispersive downlink channels," in *Proc. IEEE VTC-Fall*, Sep. 2012, pp. 1–5.

[8] M. I. Kadir, S. Sugiura, J. Zhang, S. Chen, and L. Hanzo, "OFDMA/SC-FDMA-aided space–time shift keying for dispersive multiuser scenarios," *IEEE Trans. Veh. Technol.*, vol. 62, no. 1, pp. 408–414, Jan. 2013.

[9] D. Divsalar and M. Simon, "Multiple-symbol differential detection of MPSK," *IEEE Trans. Commun.*, vol. 38, no. 3, pp. 300–308, Mar. 1990.

[10] L. Lampe, R. Schober, V. Pauli, and C. Windpassinger, "Multiple-symbol differential sphere decoding," *IEEE Trans. Commun.*, vol. 53, no. 12, pp. 1981–1985, Dec. 2005.

[11] V. Pauli and L. Lampe, "On the complexity of sphere decoding for differential detection," *IEEE Trans. Inf. Theory*, vol. 53, no. 4, pp. 1595–1603, Apr. 2007.

[12] C. Xu, S. Sugiura, S. X. Ng, and L. Hanzo, "Reduced-complexity non-coherently detected differential space–time shift keying," *IEEE Signal Process. Lett.*, vol. 18, no. 3, pp. 153–156, Mar. 2011.

[13] S. ten Brink, "Convergence behavior of iteratively decoded parallel concatenated codes," *IEEE Trans. Commun.*, vol. 49, no. 10, pp. 1727–1737, Oct. 2001.

[14] B. Hochwald and S. ten Brink, "Achieving near-capacity on a multiple-antenna channel," *IEEE Trans. Commun.*, vol. 51, no. 3, pp. 389–399, Mar. 2003.

[15] V. Pauli, L. Lampe, and R. Schober, ""Turbo DPSK" using soft multiple-symbol differential sphere decoding," *IEEE Trans. Inf. Theory*, vol. 52, no. 4, pp. 1385–1398, Apr. 2006.

[16] V. Pauli, L. Lampe, and J. Huber, "Differential space–frequency modulation and fast 2-D multiple-symbol differential detection for MIMO-OFDM," *IEEE Trans. Veh. Technol.*, vol. 57, no. 1, pp. 297–310, Jan. 2008.

[17] D. Divsalar, S. Dolinar, and F. Pollara, "Serial concatenated trellis coded modulation with rate-1 inner code," in *Proc. IEEE GLOBECOM*, Dec. 2000, vol. 2, pp. 777–782.

[18] M. Tüchler, “Design of serially concatenated systems depending on the block length,” *IEEE Trans. Commun.*, vol. 52, no. 2, pp. 209–218, Feb. 2004.
[19] L. Hanzo, O. Alamri, M. El-Hajjar, and N. Wu, *Near-Capacity Multi-Functional MIMO Systems (Sphere-Packing, Iterative Detection and Cooperation)*. New York, NY, USA: Wiley, 2009.
[20] S. Sugiura, “Dispersion matrix optimization for space–time shift keying,” *IEEE Commun. Lett.*, vol. 15, no. 11, pp. 1152–1155, Nov. 2011.
[21] S. Sugiura, “Coherent versus non-coherent space–time shift keying for co-located and distributed MIMO systems,” Ph.D. dissertation, Univ. Southampton, Southampton, U.K., 2010.
[22] M. Jiang and L. Hanzo, “Multiuser MIMO-OFDM for next-generation wireless systems,” *Proc. IEEE*, vol. 95, no. 7, pp. 1430–1469, Jul. 2007.
[23] R. H. Clarke, “A statistical theory of mobile radio reception,” *Bell Syst. Tech. J.*, vol. 47, no. 6, pp. 957–1000, Jul. 1968.
[24] V. Pauli and L. Lampe, “Tree-search multiple-symbol differential decoding for unitary space–time modulation,” *IEEE Trans. Commun.*, vol. 55, no. 8, pp. 1567–1576, Aug. 2007.
[25] E. Chiavaccini and G. Vitetta, “Further results on differential space–time modulations,” *IEEE Trans. Commun.*, vol. 51, no. 7, pp. 1093–1101, Jul. 2003.
[26] R. Schober and L. H.-J. Lampe, “Noncoherent receivers for differential space–time modulation,” *IEEE Trans. Commun.*, vol. 50, no. 5, pp. 768–777, May 2002.
[27] B. L. Hughes, “Differential space–time modulation,” *IEEE Trans. Inf. Theory*, vol. 46, no. 7, pp. 2567–2578, Nov. 2000.
[28] A. Burg, M. Borgmann, M. Wenk, M. Zellweger, W. Fichtner, and H. Bolcskei, “VLSI implementation of MIMO detection using the sphere decoding algorithm,” *IEEE J. Solid-State Circuits*, vol. 40, no. 7, pp. 1566–1577, Jul. 2005.
[29] N. Seshadri and P. Hoeher, “On post-decision symbol-reliability generation,” in *Proc. IEEE ICC*, May 1993, vol. 2, pp. 741–745.
[30] “Digital land mobile radio communications, final report,” Office for Official Publications of the European Communities, Luxembourg, Tech. Rep., 1989.
[31] M. Patzold, *Mobile Fading Channels*. New York, NY, USA: Wiley, 2003.
[32] M. El-Hajjar and L. Hanzo, “EXITcharts for system design and analysis,” *IEEE Commun. Surveys Tuts.*, vol. 16, no. 1, pp. 127–153, First Quarter 2014.
[33] J. Hagenauer, “The EXIT chart-Introduction to extrinsic information transfer in iterative processing,” in *Proc. Eur. Signal Process. Conf.*, Vienna, Austria, Sep. 2004, pp. 1541–1548.

AUTHOR QUERY

NO QUERY.

Correspondence

OFDM-Aided Differential Space–Time Shift Keying Using Iterative Soft Multiple-Symbol Differential Sphere Decoding

Mohammad Ismat Kadir, Sheng Chen, K. V. S. Hari, K. Giridhar, and Lajos Hanzo

***Abstract*—Soft-decision multiple-symbol differential sphere decoding (MSDSD) is proposed for orthogonal frequency-division multiplexing (OFDM)-aided differential space–time shift keying (DSTSK)-aided transmission over frequency-selective channels. Specifically, the DSTSK signaling blocks are generated by the channel-encoded source information and the space–time (ST) blocks are appropriately mapped to a number of OFDM subcarriers. After OFDM demodulation, the DSTSK signal is noncoherently detected by our soft-decision MSDSD detector. A novel soft-decision MSDSD detector is designed, and the associated decision rule is derived for the DSTSK scheme. Our simulation results demonstrate that an SNR reduction of 2 dB is achieved by the proposed scheme using an MSDSD window size of $N_w = 4$ over the conventional soft-decision-aided differential detection benchmarker, while communicating over dispersive channels and dispensing with channel estimation (CE).**

***Index Terms*—Extrinsic information transfer (EXIT) chart, iterative decoding, multiple-symbol differential sphere decoding (MSDSD), orthogonal frequency-division multiplexing (OFDM), space–time shift keying (STSK).**

I. Introduction

Space–time shift keying (STSK) [1]–[3] has emerged as a beneficial multiple-input–multiple-output (MIMO) concept. STSK bridges the gap between the flexible diversity–multiplexing tradeoff provided by linear dispersion codes (LDCs) [4], [5] and the low-complexity design of spatial modulation (SM) [6]. Similar to the LDCs, STSK spreads the user information to both the spatial and time dimensions, but instead of simultaneously activating all the dispersion matrices (DMs), it transmits an additional $\log_2 Q$ bits by activating one out of Q DMs. To overcome the performance degradation of the STSK scheme in wideband channels, orthogonal frequency-division multiplexing (OFDM)-aided STSK [7] and orthogonal frequency-division multiple-access /single-carrier frequency-division multiple-access-aided STSK [8] have also been proposed. The previous STSK studies [1], [2] demonstrate that coherent STSK performs well in conjunction with perfect channel state information (CSI) but exhibits a severe error floor in the presence of channel estimation (CE) errors.

Manuscript received July 27, 2013; revised December 21, 2013; accepted February 8, 2014. This work was supported in part by the Research Council U.K. under the auspices of the India–U.K. Advanced Technology Center of the European Union under the Concerto Project and in part by the European Research Council under its Advanced Fellow Grant. The review of this paper was coordinated by Prof. Y. Su.

M. I. Kadir, S. Chen, and L. Hanzo are with the School of Electronics and Computer Science, University of Southampton, Southampton SO17 1BJ, U.K. (e-mail: mik1g09@ecs.soton.ac.uk; sqc@ecs.soton.ac.uk; lh@ecs.soton.ac.uk).

K. V. S. Hari is with the Department of Electrical Communication Engineering, Indian Institute of Science, Bangalore 560012, India (e-mail: hari@ece.iisc.ernet.in).

K. Giridhar is with the Department of Electrical Engineering, Indian Institute of Technology Madras, Chennai 600036, India (e-mail: giri@tenet.res.in).

Color versions of one or more of the figures in this paper are available online at http://ieeexplore.ieee.org.

Digital Object Identifier 10.1109/TVT.2014.2306654

Differential STSK (DSTSK) employing conventional differential detection (CDD) has also been proposed for the sake of dispensing with the CE [2] and thus to eliminate the potentially high-Doppler-dependent pilot overhead. However, CDD suffers from a typical 3-dB performance penalty in low-Doppler scenarios. Furthermore, an irreducible error floor may be observed in a high-mobility scenario characterized by a high Doppler frequency. To circumvent the performance degradation of CDD, multiple-symbol differential detection (MSDD) was proposed for differential phase-shift keying (DPSK) in [9]. MSDD uses the fading-plus-noise statistics of the channel for jointly detecting $(N_w - 1)$ information symbols from N_w number of consecutively received symbols, where N_w is usually referred to as the *observation window size*. The performance improvement of MSDD is, however, achieved at the cost of increased complexity, which increases exponentially with N_w. For mitigating this potentially excessive complexity, sphere decoding (SD) was invoked for MSDD in the context of multiple-symbol differential sphere decoding (MSDSD) in [10] and [11]. Hard-decision MSDSD was conceived in [12] for a DSTSK scheme operating in nondispersive channels. As a further advance, inspired by the near-capacity performance of turbo detection [13], [14], a soft-decision MSDSD scheme was also designed for DPSK in [15]. Furthermore, the concept of differential space–frequency modulation employing MSDSD in conjunction with a specific subcarrier allocation was proposed in [16] for exploiting both the achievable spatial- and frequency-domain diversity. However, the conception of the soft-decision-MSDSD-aided DSTSK designed for realistic dispersive scenarios constitutes an unexplored open problem.

Against this background, we conceive a novel soft-decision MSDSD for OFDM-based DSTSK operating in frequency-selective channels. The main contributions of this paper are as follows.

1) A novel soft-decision-aided MSDSD is proposed for OFDM-aided DSTSK operating in dispersive channels. The decision rule of the soft-decision MSDSD is deduced by considering the construction of DSTSK codewords based on the DMs, the Doppler frequency, the OFDM system parameters, and the generation of soft information.
2) A lower bound of the detection complexity is deduced, which is verified by simulations.

The remainder of this paper is organized as follows. In Section II, an overview of the proposed channel-coded OFDM-aided DSTSK scheme is provided. The soft-decision MSDSD is modeled in Section III. In Section IV, both the complexity imposed by the system is quantified. The performance of the soft-decision MSDSD-aided DSTSK scheme is investigated in Section V. Finally, we conclude in Section VI.

Notations: We use capital boldface letters to denote matrices, whereas $\{\cdot\}^T$, $\{\cdot\}^H$, $\mathrm{tr}(\cdot)$, $\det[\cdot]$, and $\|\cdot\|$ are used to represent the transpose, the Hermitian transpose, the trace, the determinant, and the Euclidean norm of the matrix "$\cdot$," respectively. The notations $\mathcal{E}\{\cdot\}$, $\cdot^*$, and $P(\cdot)$ are used to denote the expected value, the complex conjugate, and the probability of "$\cdot$" respectively, whereas $\otimes$ and $\boldsymbol{I}_T$ represent the Kronecker product and the $(T \times T)$ identity matrix, respectively. A symmetric $(N_w \times N_w)$ Toeplitz matrix is denoted toeplitz$\{x_1, \ldots, x_{N_w}\}$, whereas $\mathrm{diag}\{\boldsymbol{X}_1, \ldots, \boldsymbol{X}_{N_w}\}$ indicates a block-diagonal matrix with the matrices $\boldsymbol{X}_1, \ldots, \boldsymbol{X}_{N_w}$ on its main diagonal. Furthermore, $\mathcal{CN}(\mu, \sigma^2)$ refers to the circularly symmetric complex Gaussian distribution with mean μ and variance σ^2.

0018-9545 © 2014 IEEE. Personal use is permitted, but republication/redistribution requires IEEE permission.
See http://www.ieee.org/publications_standards/publications/rights/index.html for more information.

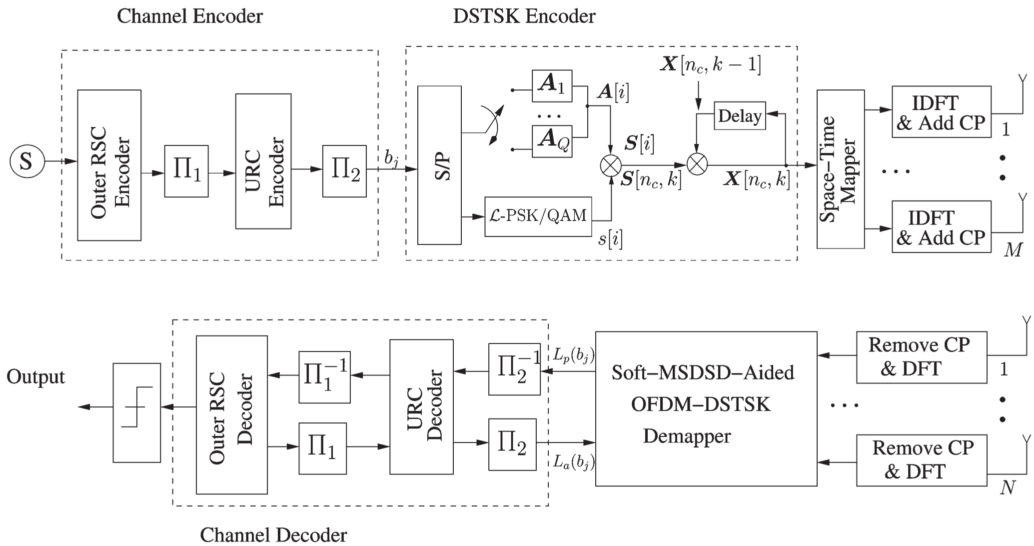

Fig. 1. Transceiver architecture of the proposed concatenated channel-coding-aided DSTSK scheme relying on the soft-decision MSDSD as the inner decoder.

II. System Model

We consider a channel-coded OFDM-aided DSTSK transceiver employing M transmit and N receive antenna elements (AEs), as shown in Fig. 1. The channel encoder/decoder blocks of Fig. 1 may incorporate a general channel coding scheme that supports soft-decision decoding at affordable complexity. A pragmatic coding architecture might be an appropriately interleaved serially concatenated recursive convolutional code (RSC) and unity rate code (URC)-aided scheme [17]–[19], as shown in Fig. 1.

The source bits are first channel encoded by the RSC code, and the encoded bits are then interleaved by a random bit interleaver Π_1. Following URC precoding, the interleaved bits are further interleaved by a second interleaver Π_2. The resultant bits are then mapped to STSK codewords, which are further mapped to N_c parallel subcarriers and then differentially encoded in the time domain (TD), i.e., across the consecutive OFDM symbols of the same subcarrier. The DSTSK codewords are then OFDM modulated, while incorporating appropriate cyclic prefixes (CPs).

The signal received is first OFDM demodulated and then input to the DSTSK soft-decision MSDSD demapper. The extrinsic soft information is then iteratively exchanged between the three soft-in–soft-out components, namely, the DSTSK demapper, the URC decoder, and the RSC decoder, before finally outputting the estimated bits [8], [19].

A. DSTSK Architecture and OFDM Layout

The STSK encoder generates space–time (ST) codewords from the source information by activating a single DM in any symbol duration in conjunction with the classic modulated symbols for transmission over T time slots using M transmit AEs [1], [2]. More specifically, each STSK signaling block $\boldsymbol{S}[i] \in \mathbb{C}^{T\times M}$ is created from $\log_2(\mathcal{L}\cdot Q)$ source bits according to [1], [2]

$$\boldsymbol{S}[i] = s[i]\boldsymbol{A}[i] \tag{1}$$

where $s[i]$ is an $\mathcal{L}$-ary constellation symbol represented by $\log_2 \mathcal{L}$ bits, and $\boldsymbol{A}[i] \in \mathbb{C}^{T\times M}$ is the specific DM activated from the set of Q DMs $\boldsymbol{A}_q(q = 1, \ldots, Q)$, as determined by the remaining $\log_2 Q$ bits. The DMs $\boldsymbol{A}_q(q = 1, \ldots, Q)$ are unitary matrices generated by employing an exhaustive search for minimizing the objective function constituted by the pairwise error probability of the codewords [5], [12], [20], [21] under the power constraint in [2] expressed by $\mathrm{tr}(\boldsymbol{A}_q^H \boldsymbol{A}_q) = T\,\forall\, q$. The resultant STSK system is then uniquely and unambiguously described by the parameters $(M, N, T, Q, \mathcal{L})$.

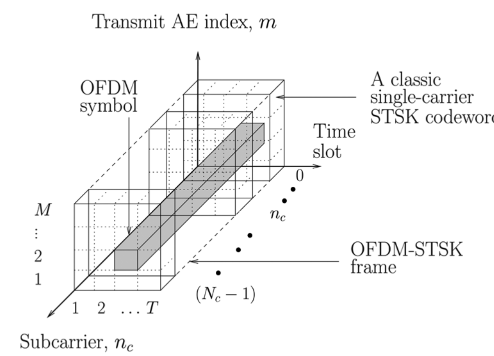

Fig. 2. Mapping of the STSK codewords to N_c parallel OFDM subcarriers showing the construction of an OFDM-STSK frame and OFDM symbols. After being appropriately mapped to the subcarriers, the codewords are differentially encoded in the TD and transmitted over dispersive channels by M transmit AEs over T time-slots.

We observe that the STSK codeword $\boldsymbol{S}[i]$ belongs to a set $\boldsymbol{\mathcal{S}}$ of $(\mathcal{L}\cdot Q)$ codeword matrices defined by

$$\boldsymbol{\mathcal{S}} \triangleq \{s_l \boldsymbol{A}_q | \,(q \in \{1, \ldots, Q\}, \quad l \in \{1, \ldots, \mathcal{L}\})\}. \tag{2}$$

The STSK codewords are mapped to N_c parallel subcarriers, as shown in Fig. 2, before being differentially encoded. As shown in Fig. 2, N_c consecutive STSK codewords are arranged in parallel to form an OFDM-STSK frame, and OFDM modulation is carried out over each shaded symbol pipe, which constitutes an OFDM symbol. We may represent the codeword $\boldsymbol{S}[i]$ by $\boldsymbol{S}[n_c, k]$, so that the overall codeword index i is related to the OFDM frame index k and the subcarrier index n_c by $i = kN_c + n_c$, $n_c = 0, 1, \ldots, (N_c - 1)$. Additionally, we invoke differential encoding in the TD, i.e., differential encoding is performed across the consecutive OFDM symbols of the same subcarrier. We have chosen TD differential encoding/decoding because we have conceived our scheme for continuous transmissions, as opposed to the FD differential encoding/decoding across adjacent FD subcarriers, which is more suitable for burst transmissions. To facilitate convenient differential encoding, we assume $M = T$. Furthermore, directly generated unitary DMs are used in the proposed scheme for avoiding the nonlinear Cayley transform [2], [12]. The codewords

$\boldsymbol{S}[n_c, k]$ are thus differentially encoded to form the transmit blocks $\boldsymbol{X}[n_c, k]$ $(k = 0, 1, 2, \ldots)$ according to [16]

$$\boldsymbol{X}[n_c, k] = \begin{cases} \boldsymbol{X}[n_c, k-1]\boldsymbol{S}[n_c, k], & k = 1, 2, \ldots \\ \boldsymbol{I}_T & k = 0. \end{cases} \quad (3)$$

The DSTSK codewords are then transmitted after the N_c-point inverse discrete Fourier transform (DFT) operation and appropriate CP incorporation.

B. Channel Model

Each link between the mth transmit and nth receive AE is assumed a frequency-selective channel, but as a benefit of OFDM-based transmission, each dispersive channel is then partitioned into N_c low-rate parallel frequency-flat subchannels [22]. The complex-valued fading gain $h_{m,n}[n_c, k]$ $(m = 1, 2, \ldots, M;\ n = 1, 2, \ldots, N)$ obeys the distribution $\mathcal{CN}(0, 1)$ associated with an autocorrelation function based on Clarke's model [23]: $\varphi_{hh}[n_c, \kappa] \triangleq \mathcal{E}\{h_{m,n}[n_c, k]h^*_{m,n}[n_c, k+\kappa]\} = J_0(2\pi\kappa f_d)$, where J_0 denotes the zeroth-order Bessel function of the first kind, and $f_d = f_m\mathcal{T}$ is the normalized maximum Doppler frequency, whereas f_m and $1/\mathcal{T}$ represent the maximum Doppler frequency and the symbol rate, respectively. The fading is assumed quasi-static, i.e., the channel's complex-valued envelope remains approximately constant during the transmission of an OFDM STSK frame.

Given the aforementioned assumptions, the received signal $\boldsymbol{Y}[n_c, k] \in \mathbb{C}^{T\times N}$ obtained after CP removal and DFT may be expressed by [16], [22]

$$\boldsymbol{Y}[n_c, k] = \boldsymbol{X}[n_c, k]\boldsymbol{H}[n_c, k] + \boldsymbol{V}[n_c, k] \quad (4)$$

where $\boldsymbol{X}[n_c, k] \in \mathbb{C}^{T\times M}$ represents the codeword transmitted and $\boldsymbol{H}[n_c, k] \in \mathbb{C}^{M\times N}$ denotes the FD channel transfer matrix, with its (m, n)th entry given by $h_{m,n}[n_c, k]$. Furthermore, $\boldsymbol{V}[n_c, k] \in \mathbb{C}^{T\times N}$ is the additive white Gaussian noise (AWGN) with entries of $v_{T_i,n}[n_c, k] \sim \mathcal{CN}(0, \sigma_n^2)$.

III. MSDSD Receiver

This section introduces the maximum-likelihood MSDSD (ML-MSDSD), the maximum *a posteriori* MSDSD (MAP-MSDSD) algorithm, and the generation of the log-likelihood ratios (LLRs) for the soft-decision-MSDSD-aided OFDM DSTSK.

A. ML-MSDSD for OFDM-Aided DSTSK

The ML-MSDD processes N_w consecutively received space–time blocks corresponding to the n_cth subcarrier given by $\bar{\boldsymbol{Y}}[n_c, k] \triangleq [\boldsymbol{Y}^T[n_c, k-N_w+1], \ldots, \boldsymbol{Y}^T[n_c, k]]^T$ and finds the ML estimates $\hat{\bar{\boldsymbol{X}}}[n_c, k]$ of the corresponding N_w transmitted blocks $\bar{\boldsymbol{X}}[n_c, k] \triangleq [\boldsymbol{X}^T[n_c, k-N_w+1], \ldots, \boldsymbol{X}^T[n_c, k]]^T$ [24]. Since the differentially encoded blocks $\boldsymbol{X}[n_c, k]$ are related to the STSK codewords by the one-to-one relationship expressed by (3), the ML-MSDD in turn estimates $(N_w - 1)$ STSK codewords given by $\bar{\boldsymbol{S}}[n_c, k] \triangleq [\boldsymbol{S}^T[n_c, k-N_w+2], \ldots, \boldsymbol{S}^T[n_c, k]]^T$, which further estimates the source bits mapped to the STSK codewords.

Defining a block-diagonal matrix $\bar{\boldsymbol{X}}_D[n_c, k]$ by $\bar{\boldsymbol{X}}_D[n_c, k] \triangleq \mathrm{diag}\{\boldsymbol{X}[n_c, k-N_w+1], \ldots, \boldsymbol{X}[n_c, k]\}$, $\bar{\boldsymbol{H}}[n_c, k] \triangleq [\boldsymbol{H}^T[n_c, k-N_w+1], \ldots, \boldsymbol{H}^T[n_c, k]]^T$, and $\bar{\boldsymbol{V}}[n_c, k] \triangleq [\boldsymbol{V}^T[n_c, k-N_w+1], \ldots, \boldsymbol{V}^T[n_c, k]]^T$, the N_w-block received sequence can be expressed by [11], [24]

$$\bar{\boldsymbol{Y}}[n_c, k] = \bar{\boldsymbol{X}}_D[n_c, k]\bar{\boldsymbol{H}}[n_c, k] + \bar{\boldsymbol{V}}[n_c, k] \quad (5)$$

where

$$\bar{\boldsymbol{Y}}[n_c, k] \in \mathbb{C}^{N_wM\times N} \quad \bar{\boldsymbol{V}}[n_c, k] \in \mathbb{C}^{N_wM\times N}$$
$$\bar{\boldsymbol{H}}[n_c, k] \in \mathbb{C}^{N_wM\times N} \quad \bar{\boldsymbol{X}}_D[n_c, k] \in \mathbb{C}^{N_wM\times N_wM}.$$

For the sake of notational simplicity, we omit the subcarrier index and time index $[n_c, k]$ in the following and refer to the μth submatrix of a block matrix, e.g., $\boldsymbol{B}$ by the subscripted matrix $\boldsymbol{B}_\mu$. Under the assumption that $h_{m,n}$ and $v_{T_i,n}$ $(m = T_i = 1, 2, \ldots, M, n = 1, 2, \ldots, N)$ are zero-mean Gaussian random processes, the probability density function of $\bar{\boldsymbol{Y}}$ conditioned on $\bar{\boldsymbol{X}}_D$ is given by [25], [26]

$$P(\bar{\boldsymbol{Y}}|\bar{\boldsymbol{X}}_D) = \frac{1}{(\pi^{N_wM}\det[\boldsymbol{\Lambda}_Y])^N}\exp\left\{-\mathrm{tr}\left(\bar{\boldsymbol{Y}}^H\boldsymbol{\Lambda}_Y^{-1}\bar{\boldsymbol{Y}}\right)\right\} \quad (6)$$

where $\boldsymbol{\Lambda}_Y$ is defined by $\boldsymbol{\Lambda}_Y \triangleq \mathcal{E}\{\bar{\boldsymbol{Y}}\bar{\boldsymbol{Y}}^H|\bar{\boldsymbol{X}}_D\}$. The ML estimate $\hat{\bar{\boldsymbol{X}}}$ under the assumption of quasi-static fading and unitary $\bar{\boldsymbol{X}}_D$ reduces to [26], [27]

$$\hat{\bar{\boldsymbol{X}}} = \arg\max_{\tilde{\bar{\boldsymbol{X}}}} P(\bar{\boldsymbol{Y}}|\bar{\boldsymbol{X}}_D) = \arg\min_{\tilde{\bar{\boldsymbol{X}}}}\left\{\mathrm{tr}\left(\bar{\boldsymbol{Y}}^H\boldsymbol{\Lambda}_Y^{-1}\bar{\boldsymbol{Y}}\right)\right\}. \quad (7)$$

Here, the conditional covariance matrix $\boldsymbol{\Lambda}_Y$ is related to the channel parameters [25], [26] by

$$\boldsymbol{\Lambda}_Y^{-1} = \frac{1}{N}\bar{\boldsymbol{X}}_D(\boldsymbol{\Lambda}^{-1}\otimes\boldsymbol{I}_M)\bar{\boldsymbol{X}}_D^H \quad (8)$$

where we have $\boldsymbol{\Lambda} \triangleq (\boldsymbol{\psi}_{hh}+\sigma_n^2\boldsymbol{I}_{N_w})$ and $\boldsymbol{\psi}_{hh} \triangleq \mathtt{toeplitz}\{\varphi_{hh}[n_c, 0], \ldots, \varphi_{hh}[n_c, (N_w-1)]\}$, with the component autocorrelation functions $\varphi_{hh}[n_c, \kappa]$ being identical for all spatial channels. Applying the Cholesky factorization of $\boldsymbol{\Lambda}^{-1} = \boldsymbol{U}^H\boldsymbol{U}$ with the upper triangular matrix $\boldsymbol{U}$ and considering the identity $\mathrm{tr}(\boldsymbol{\mathcal{X}}\boldsymbol{\mathcal{X}}^H) = \|\boldsymbol{\mathcal{X}}\|^2$ for any matrix $\boldsymbol{\mathcal{X}}$, the ML-MSDD decision rule can be deduced from (6), yielding [11]

$$\hat{\bar{\boldsymbol{X}}} = \arg\min_{\tilde{\bar{\boldsymbol{X}}}}\left\{\sum_{\mu=1}^{N_w}\left\|\boldsymbol{Y}^H_{\mu,\mu}\tilde{\boldsymbol{X}}_\mu + \sum_{\nu=\mu+1}^{N_w}\left(\boldsymbol{Y}^H_{\mu,\nu}\tilde{\boldsymbol{X}}_\nu\right)\right\|^2\right\} \quad (9)$$

where $\boldsymbol{Y}^H_{\mu,\nu}$ is defined by $\boldsymbol{Y}^H_{\mu,\nu} \triangleq \boldsymbol{Y}_\nu u_{\mu,\nu}$, and $u_{\mu,\nu}$ represents the (μ, ν)th element of $\boldsymbol{U}$. Still referring to (9), $\hat{\bar{\boldsymbol{X}}}$ denotes the *estimate* of $\bar{\boldsymbol{X}}_D$, whereas $\tilde{\boldsymbol{X}}_\mu$ refers to the μth *candidate* submatrix of $\bar{\boldsymbol{X}}_D$.

Since the ML metric of (9) is invariant to a phase shift common to all elements of $\tilde{\boldsymbol{X}}_\mu\ \forall\mu$ corresponding to the same $\bar{\boldsymbol{S}}$ (where $\boldsymbol{S}^T_\lambda \in \boldsymbol{\mathcal{S}}\,\forall\lambda$), the accumulated differential matrices may be expressed as [15]

$$\boldsymbol{\mathcal{A}}_\nu = \begin{cases} \prod_{\lambda=\nu}^{N_w-1}\boldsymbol{S}^H_\lambda, & 1 \leqslant \nu \leqslant (N_w-1) \\ \boldsymbol{I}_T, & \nu = N_w. \end{cases} \quad (10)$$

For the sake of reducing the complexity associated with an exhaustive search, we employ MSDSD similar to [10] and [11] to search through the candidate set lying within a sphere of radius ρ_s as follows:

$$\sum_{\mu=1}^{N_w}\left\|\boldsymbol{Y}^H_{\mu,\mu}\boldsymbol{A}_\mu + \sum_{\nu=\mu+1}^{N_w}\left(\boldsymbol{Y}^H_{\mu,\nu}\boldsymbol{\mathcal{A}}_\nu\right)\right\|^2 \leq \rho_s^2. \quad (11)$$

B. MAP-MSDSD

Assuming the STSK codewords to be mutually independent, (6) and (9) yield [15]:

$$\begin{aligned} &-\ln\left(P(\bar{\boldsymbol{S}}|\bar{\boldsymbol{Y}})\right) \\ &\quad\propto -\ln\left(P(\bar{\boldsymbol{Y}}|\bar{\boldsymbol{S}})\right) - \ln\left(P(\bar{\boldsymbol{S}})\right) \\ &\quad\propto \sum_{\mu=1}^{N_w}\left\{\left\|\boldsymbol{Y}^H_{\mu,\mu}\boldsymbol{\mathcal{A}}_\mu + \sum_{\nu=\mu+1}^{N_w}\boldsymbol{Y}^H_{\mu,\nu}\boldsymbol{\mathcal{A}}_\nu\right\|^2 - \ln\left(P(\boldsymbol{S}_\mu)\right)\right\}. \quad (12) \end{aligned}$$

The MAP-MSDSD may be thus expressed as

$$\sum_{\mu=1}^{(N_w-1)}\left(\left\|\sum_{\nu=\mu}^{N_w}\left(\boldsymbol{Y}_{\mu,\,\nu}^{H}\boldsymbol{\mathcal{A}}_\nu\right)\right\|^2-\ln\left(P(\boldsymbol{S}_\mu)\right)\right)$$
$$\leq \rho_s^2-\|u_{N_w,N_w}\boldsymbol{Y}_{N_w}\|^2\triangleq\rho^2. \quad (13)$$

Clearly, the codeword $\boldsymbol{S}_\mu$ obeys the specific distance criterion [10], [12], [28] that the current partial Euclidean distance (PED) d_μ^2 is the sum of the previous PED $d_{\mu+1}^2$ and the distance increment $\triangle_\mu^2$, i.e.,

$$\begin{aligned} d_\mu^2 &\triangleq \triangle_\mu^2+d_{\mu+1}^2\\ &=\left\|u_{\mu,\mu}\boldsymbol{Y}_\mu\boldsymbol{\mathcal{A}}_{\mu+1}\boldsymbol{S}_\mu^H+\sum_{\nu=\mu+1}^{N_w}u_{\mu,\,\nu}\boldsymbol{Y}_\nu\boldsymbol{\mathcal{A}}_\nu\right\|^2-\ln\left(P(\boldsymbol{S}_\mu)\right)\\ &\quad+\sum_{\iota=\mu+1}^{(N_w-1)}\left(\left\|\sum_{\nu=\iota}^{N_w}u_{\iota,\nu}\boldsymbol{Y}_\nu\boldsymbol{\mathcal{A}}_\nu\right\|^2-\ln\left(P(\boldsymbol{S}_\iota)\right)\right)\leq\rho^2. \quad (14)\end{aligned}$$

Similar to the MSDSD principle described in [10] and [15], the MAP-MSDSD is initialized with $\mu=(N_w-1)$ and then proceeds by applying the search criterion of (14) until $\mu=1$, where the search radius is updated to $\rho^2=d_1^2$, and the search is repeated by commencing from $\mu=2$ until $\mu=(N_w-1)$ is reached. If the new search does not provide a better estimate, the previous estimate is retained.

C. Log-Likelihood Ratio and Soft-Decision-MSDSD-Aided OFDM DSTSK

The soft demapper relies on the *a priori* information gleaned from the URC decoder and the MAP-MSDSD. A high interleaver depth is assumed so that the permuted bits may be treated as being independent. The LLR corresponding to the bit b_j interleaved by the interleaver Π_2 of Fig. 1 is defined by [29] $L_a(b_j)\triangleq\ln(P(b_j=b)/P(b_j=\bar{b}))$, where $b\in\{0,1\}$, and the jth bit $b_j=b$ corresponds to the MAP-MSDSD estimate $\hat{\hat{\boldsymbol{S}}}$, whereas $\bar{b}$ indicates its complement. The *a posteriori* LLR $L_p(\cdot)$ of b_j may be then approximated by the maximum-logarithmic-MAP (max-log-MAP) algorithm [14], [15], i.e.,

$$\begin{aligned} &L_p(b_j)\\ &=\ln\frac{P(b_j=b|\boldsymbol{Y})}{P(b_j=\bar{b}|\boldsymbol{Y})}\\ &\approx\ln\frac{\max_{\bar{\boldsymbol{S}}:b_j=b}\left[-\sum_{\mu=1}^{N_w}\left\|\sum_{\nu=\mu}^{N_w}\left(\boldsymbol{Y}_{\mu,\,\nu}^H\hat{\boldsymbol{\mathcal{A}}}_\nu\right)\right\|^2+\ln\left(P(\hat{\hat{\boldsymbol{S}}})\right)\right]}{\max_{\bar{\boldsymbol{S}}:b_j=\bar{b}}\left[-\sum_{\mu=1}^{N_w}\left\|\sum_{\nu=\mu}^{N_w}\left(\boldsymbol{Y}_{\mu,\,\nu}^H\hat{\boldsymbol{\mathcal{A}}}_\nu\right)\right\|^2+\ln\left(P(\hat{\hat{\boldsymbol{S}}})\right)\right]}\\ &=-\sum_{\mu=1}^{N_w}\left\|\sum_{\nu=\mu}^{N_w}\left(\boldsymbol{Y}_{\mu,\,\nu}^H\hat{\boldsymbol{\mathcal{A}}}_\nu^b\right)\right\|^2+\ln\left(P(\hat{\hat{\boldsymbol{S}}}^b)\right)\\ &\quad+\sum_{\mu=1}^{N_w}\left\|\sum_{\nu=\mu}^{N_w}\left(\boldsymbol{Y}_{\mu,\,\nu}^H\hat{\boldsymbol{\mathcal{A}}}_\nu^{\bar{b}}\right)\right\|^2-\ln\left(P(\hat{\hat{\boldsymbol{S}}}^{\bar{b}})\right) \quad (15)\end{aligned}$$

where $\hat{\hat{\boldsymbol{S}}}^b$ and $\hat{\hat{\boldsymbol{S}}}^{\bar{b}}$ represent the MAP-MSDSD estimate and the constrained estimate associated with $b_j=\bar{b}$, respectively.

The extrinsic LLR $L_e(\cdot)$ for b_j is now evaluated by combining the *a posteriori* and *a priori* LLR: $L_e(b_j)=L_p(b_j)-L_a(b_j)$. The extrinsic information extracted from the soft-decision MSDSD demapper is iteratively exchanged with the URC decoder of Fig. 1, which forms the *inner* iteration, whereas the exchange of extrinsic information between the URC decoder and the RSC decoder of Fig. 1 may be termed as the *outer* iteration. Note that, for each outer iteration between the RSC decoder and the URC decoder, several inner iterations may be invoked between the URC and the soft-decision-MSDSD-aided DSTSK demapper [2], [19]. Finally, the RSC decoder generates *a posteriori* LLRs, from which the source bits are estimated.

IV. Complexity

Here, the complexity of the proposed scheme is detailed, and the complexity imposed by the MAP-MSDSD is quantified.

Equation (2) shows that there exists $(\mathcal{L}\cdot Q)$ legitimate codeword matrices for each $\log_2(\mathcal{L}\cdot Q)$ bits of source information. The exhaustive-search-based solution to (9) involves a search in a $(\mathcal{L}\cdot Q)^{(N_w-1)}$ element space of candidate matrices $\tilde{\boldsymbol{X}}$ corresponding to all possible choices of $\tilde{\boldsymbol{S}}$. The ML-MSDSD associated with chosen sphere radius ρ imposes average complexity, which is lower bounded by [11]

$$C\geq\frac{(\mathcal{L}\cdot Q)^{N_w\zeta-1}-(\mathcal{L}\cdot Q)}{(\mathcal{L}\cdot Q)-1} \quad (16)$$

where

$$\zeta\triangleq\frac{\sigma_n^2(1+\epsilon)}{2\left(1+\sigma_n^2\right)}\quad\rho^2=(1+\epsilon)NMN_w,\quad\epsilon>0. \quad (17)$$

To quantify the complexity of the MAP-MSDSD scheme, we consider the number of real-valued multiplication operations (RMOs) required for obtaining a single soft-output value, which is used as our complexity metric. The lower bound of the complexity may be obtained if the number of RMOs required for computing the soft outputs corresponding to the first codeword estimate $\hat{\hat{\boldsymbol{S}}}^b$ is counted and if a single constrained estimate $\hat{\hat{\boldsymbol{S}}}^{\bar{b}}$ is taken into account [15]. Considering the upper diagonal nature of the matrix $\boldsymbol{U}$, we observe that $\boldsymbol{Y}_{\mu,\,\nu}^H$ is defined only for $\nu\geq\mu$ in the context of (9), although each $\boldsymbol{Y}_{\mu,\,\nu}^H$ is an $(N\times T)$-element matrix, where $T=M$. The computation of the $\boldsymbol{Y}_{\mu,\,\nu}^H$ terms in (15) thus involves a total of $2MN[1+2+\cdots+N_w]=MNN_w(N_w+1)$ RMOs, assuming real-valued autocorrelation functions of $\varphi_{hh}[n_c,\,\kappa]$. To compute the *a posteriori* LLRs given by (15), the number of RMOs associated with the computation of each $\|\sum_{\nu=\mu}^{N_w}(\boldsymbol{Y}_{\mu,\,\nu}^H\hat{\boldsymbol{\mathcal{A}}}_\nu^b)\|^2$ is $4M^2N(N_w-\mu+1)+2$. The number of RMOs required for generating $\log_2(\mathcal{L}\cdot Q)$ soft outputs corresponding to a single codeword estimate $\hat{\hat{\boldsymbol{S}}}^b$ is thus given by

$$\begin{aligned}\text{RMO}[\hat{\hat{\boldsymbol{S}}}^b]&=MNN_w(N_w+1)+\sum_{\mu=1}^{N_w}\left[4M^2N(N_w-\mu+1)+2\right]\\ &=MN(2M+1)N_w(N_w+1)+2N_w. \quad (18)\end{aligned}$$

On the other hand, the number of RMOs related to each bit $\bar{b}$ of the constrained estimate $\hat{\hat{\boldsymbol{S}}}^{\bar{b}}$ is found to be $2N_w[M^2N(N_w+1)+1]$. The lower bound for the number of RMOs associated with the generation of a single soft output is thus $[MN(2M+1)/\log_2(\mathcal{L}\cdot Q)+2M^2N]N_w^2$ for large N_w. The complexity of the scheme, however, depends on a number of parameters, such as on the channel SNR, on the autocorrelation function of the channel's fading plus noise, and most importantly, on the *a priori* mutual information I_A of the inner decoder [15]. In Section V, the complexity of the MAP-MSDSD will be investigated as a function of the observation window width N_w parameterized by the available *a priori* information I_A.

TABLE I
ADOPTED VALUES OF MAIN SIMULATION PARAMETERS

Parameter	*Value*
Dispersive channel model	COST207-TU12
Fast fading envelope	Correlated Rayleigh fading
Normalized Doppler spread, f_d	0.01
Number of subcarriers, N_c	128
Length of cyclic prefix	32
Overall symbol duration	300 ns
STSK $(M, N, T, Q, \mathcal{L})$	$(2, 2, 2, 4, 4)$
RSC encoder and decoder	Half rate
	Constraint length=2
Generator polynomial	$(011, 010)_2$
Length of interleavers	$200,000$ bits
Outer iterations	11
Inner iterations	2

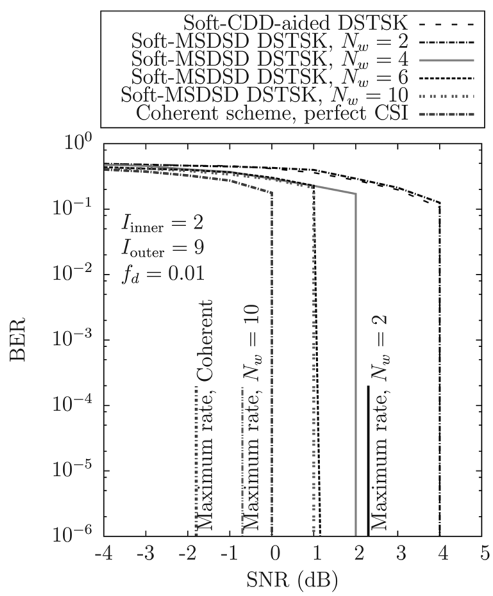

Fig. 3. Simulated BER performance of the soft-decision-MSDSD-aided OFDM DSTSK (2, 2, 2, 4, 4) scheme for transmission over dispersive COST207-TU12 channel with normalized Doppler frequency $f_d = 0.01$ and different observation window size $N_w = 2, 4, 6, 10$. The BER falls sharply after $I_{\text{outer}} = 9$ outer iterations as a benefit of employing the URC and the performance approaches that of the coherent scheme with perfect CSI with an increasing value of N_w.

V. PERFORMANCE RESULTS

Here, the performance of the proposed scheme is investigated using the parameters listed in Table I. We have employed the COST207-TU12 channel model for the links between each transmit–receive antenna pair. The power delay profile characterizing the 12 taps of the COST207-TU12 channel is detailed in [30] and [31]. As mentioned in Table I, we employ an RSC (2, 1, 2) outer code having octally represented generator polynomials of $(g_r,\ g) = (3, 2)_8$ as well as two random interleavers with a length of 200 000 bits.

Fig. 3 characterizes the achievable bit error rate (BER) of the proposed soft-decision-MSDSD-aided OFDM DSTSK scheme associated with observation window sizes of $N_w = 2, 4, 6, 10$ and compares to that achievable by the corresponding coherent scheme relying on perfect CSI. We observe that the proposed scheme has the benefit of dispensing with CE due to differential encoding, while mitigating the performance erosion of classic STSK by employing OFDM. Furthermore, the multiple-symbol detection partially mitigates the inherent performance penalty imposed by noncoherent detection. We observe in Fig. 3 that, as N_w increases, the BER performance gradually approaches that of the perfect CSI-oriented coherent scheme. Note that all the performance characteristics exhibit a vanishingly low BER after $I_{\text{outer}} = 9$ outer iterations, which is the explicit benefit of using the URC in the system. The URC is a low-complexity code, which has an infinite impulse response and hence assists the inner decoder in efficiently spreading the soft information [2], [19]. As a result, the extrinsic information transfer (EXIT) charts of Figs. 4 and 5 converge to the (1.0, 1.0) point of perfect decoding convergence, leading to a vanishingly low BER, thus eliminating the system's error floor. The maximum achievable rates for the corresponding scheme, where the scheme still exhibits an infinitesimally low BER were computed by exploiting the area property of EXIT charts [18], [32], [33] and are shown in Fig. 3 as the ultimate benchmark of the scheme.

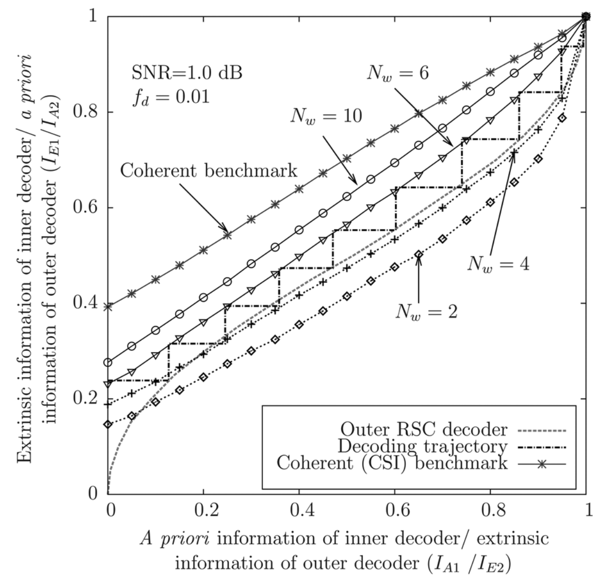

Fig. 4. EXIT charts of the inner decoders of the soft-decision-MSDSD-aided OFDM DSTSK (2, 2, 2, 4, 4) scheme at SNR $= 1$ dB with normalized Doppler frequency $f_d = 0.01$ and different observation window sizes $N_w = 2, 4, 6, 10$ and of the corresponding coherent system having perfect CSI at the receiver. At this SNR, we observe the inner EXIT charts with $N_w = 6, 10$ have an open EXIT tunnel and converge to the (1.0, 1.0) point of perfect convergence, indicating a sharp fall in the BER curve after $I_{\text{outer}} = 9$ outer iterations, which is confirmed by the decoding trajectory for $N_w = 6$. The EXIT charts with $N_w = 2, 4$ are, however, "pinched off"; thus, the BER at this SNR do not converge.

To elaborate further, Figs. 4 and 5 portray the EXIT charts of our proposed scheme at SNR $= 1$ and 4 dB, respectively. We observe in Fig. 4 that the inner decoder's EXIT charts recorded at SNR $= 1$ dB for $N_w = 2, 4$ are "pinched off," i.e., there remains no "open" EXIT tunnel, indicating a high residual BER. By contrast, the BER associated with $N_w = 6, 10$ may be expected to decrease sharply at this SNR after $I_{\text{outer}} = 9$ outer iterations, which is confirmed by the staircase-shaped Monte Carlo-simulation-based decoding trajectory [8], [13]. Fig. 5, on the other hand, shows the EXIT charts at SNR $= 4$ dB, where all the curves associated with $N_w = 2, 4, 6, 10$ exhibit an open EXIT tunnel, implying an infinitesimally low BER after $I_{\text{outer}} = 9$ iterations. The EXIT charts of the soft-decision-MSDSD-aided OFDM DSTSK recorded both for SNR $= 1$ dB and SNR $= 4$ dB are further compared in Figs. 4 and 5 to the ultimate benchmark of the coherent detector assuming perfect CSI at the receiver.

Fig. 6 characterizes the complexity associated with the MAP-MSDSD of the OFDM-aided DSTSK (2, 2, 2, 4, 4) scheme at SNR $=$ 4 dB as a function of the window size N_w, parameterized by the

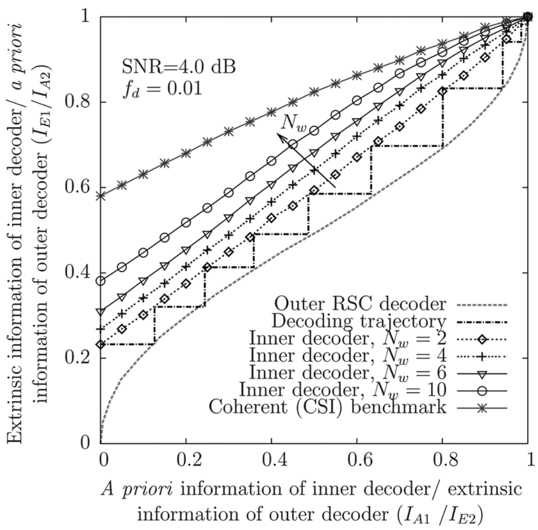

Fig. 5. EXIT charts of the inner decoders of the soft-decision-MSDSD-aided OFDM DSTSK (2, 2, 2, 4, 4) scheme at SNR = 4 dB with normalized Doppler frequency $f_d = 0.01$ and different observation window sizes $N_w = 2, 4, 6, 10$ and that of the corresponding coherent inner decoder as a benchmark. All the EXIT charts have a quite open EXIT tunnel at this SNR and converge to the (1.0, 1.0) point as a benefit of employing the URC, indicating a sharp fall in the BER curve after $I_{\text{outer}} = 9$ outer iterations, which is confirmed by the decoding trajectory.

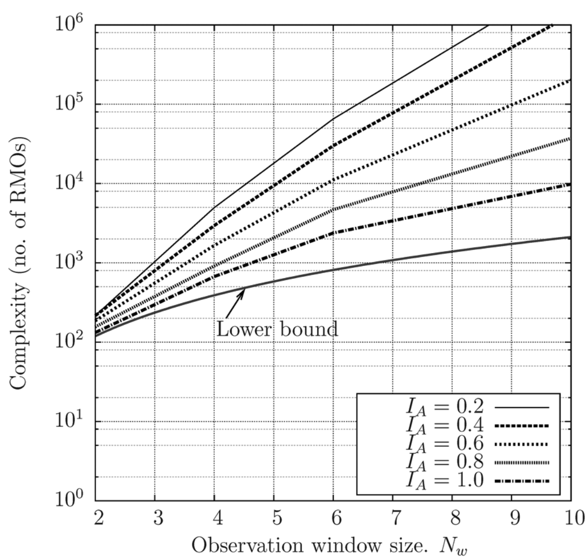

Fig. 6. Complexity in terms of the numbers of RMOs for the proposed DSTSK (2, 2, 2, 4, 4) scheme at SNR = 4 dB using the parameters of Table I as a function of observation window size N_w parameterized against the *a priori* mutual information of the inner decoder I_A. The complexity shoots up with $N_w > 6$, although the rate of increase in complexity slows down with increased *a priori* information.

a priori information I_A provided by the outer decoder for the demapper of Fig. 1. The *a priori* information I_A is measured by the average mutual information [13] between the *a priori* LLR $L_a(b_j)$ and the *a posteriori* LLR $L_p(b_j)$ of Fig. 1. The influence of the *a priori* information I_A on the complexity may be beneficially exploited in the context of adaptive system design [15], where N_w may be adaptively selected depending on the quality of the soft input. To be specific, the value of I_A increases during the consecutive decoding iterations, and we can flexibly increase N_w when the value of I_A is higher. The theoretical lower bound of the complexity quantified by the number of RMOs in Section IV is also shown as a benchmarker in Fig. 6. As expected, the complexity rapidly escalates upon increasing N_w, albeit it does not become excessively high, provided that the *a priori* information gleaned from the outer decoder is in the range of $I_A \geq 0.8$.

VI. Conclusion

We have proposed a soft-decision-MSDSD-aided multicarrier DSTSK scheme for communications over wideband channels. The OFDM-aided DSTSK provides a flexible diversity versus multiplexing gain tradeoff by spreading the source information across both the spatial and time dimensions, while mitigating the potential performance degradation imposed by the frequency selectivity of the channel. The turbo-principle-based soft-decision MSDSD facilitates joint decisions over a number of DSTSK codewords, while exploiting the fading-plus-noise statistics of the channel. We have demonstrated that the proposed soft-decision-MSDSD-aided DSTSK scheme provides substantial flexibility at moderate complexity owing to dispensing with CE. Furthermore, the MSDSD mitigates the performance degradation inflicted by the CDD scheme without an undue increase in computational complexity.

References

[1] S. Sugiura, S. Chen, and L. Hanzo, "A universal space–time architecture for multiple-antenna aided systems," *IEEE Commun. Surveys Tuts.*, vol. 14, no. 2, pp. 401–420, Second Quarter, 2012.
[2] S. Sugiura, S. Chen, and L. Hanzo, "Coherent and differential space–time shift keying: A dispersion matrix approach," *IEEE Trans. Commun.*, vol. 58, no. 11, pp. 3219–3230, Nov. 2010.
[3] S. Sugiura, S. Chen, and L. Hanzo, "Generalized space–time shift keying designed for flexible diversity-, multiplexing- and complexity-tradeoffs," *IEEE Trans. Wireless Commun.*, vol. 10, no. 4, pp. 1144–1153, Apr. 2011.
[4] B. Hassibi and B. M. Hochwald, "High-rate codes that are linear in space and time," *IEEE Trans. Inf. Theory*, vol. 48, no. 7, pp. 1804–1824, Jul. 2002.
[5] R. W. Heath, Jr. and A. Paulraj, "Linear dispersion codes for MIMO systems based on frame theory," *IEEE Trans. Signal Process.*, vol. 50, no. 10, pp. 2429–2441, Oct. 2002.
[6] R. Mesleh, H. Haas, S. Sinanovic, C. W. Ahn, and S. Yun, "Spatial modulation," *IEEE Trans. Veh. Technol.*, vol. 57, no. 4, pp. 2228–2241, Jul. 2008.
[7] M. Driusso, F. Babich, M. I. Kadir, and L. Hanzo, "OFDM aided space–time shift keying for dispersive downlink channels," in *Proc. IEEE VTC-Fall*, Sep. 2012, pp. 1–5.
[8] M. I. Kadir, S. Sugiura, J. Zhang, S. Chen, and L. Hanzo, "OFDMA/SC-FDMA-aided space–time shift keying for dispersive multiuser scenarios," *IEEE Trans. Veh. Technol.*, vol. 62, no. 1, pp. 408–414, Jan. 2013.
[9] D. Divsalar and M. Simon, "Multiple-symbol differential detection of MPSK," *IEEE Trans. Commun.*, vol. 38, no. 3, pp. 300–308, Mar. 1990.
[10] L. Lampe, R. Schober, V. Pauli, and C. Windpassinger, "Multiple-symbol differential sphere decoding," *IEEE Trans. Commun.*, vol. 53, no. 12, pp. 1981–1985, Dec. 2005.
[11] V. Pauli and L. Lampe, "On the complexity of sphere decoding for differential detection," *IEEE Trans. Inf. Theory*, vol. 53, no. 4, pp. 1595–1603, Apr. 2007.
[12] C. Xu, S. Sugiura, S. X. Ng, and L. Hanzo, "Reduced-complexity non-coherently detected differential space–time shift keying," *IEEE Signal Process. Lett.*, vol. 18, no. 3, pp. 153–156, Mar. 2011.
[13] S. ten Brink, "Convergence behavior of iteratively decoded parallel concatenated codes," *IEEE Trans. Commun.*, vol. 49, no. 10, pp. 1727–1737, Oct. 2001.
[14] B. Hochwald and S. ten Brink, "Achieving near-capacity on a multiple-antenna channel," *IEEE Trans. Commun.*, vol. 51, no. 3, pp. 389–399, Mar. 2003.
[15] V. Pauli, L. Lampe, and R. Schober, ""Turbo DPSK" using soft multiple-symbol differential sphere decoding," *IEEE Trans. Inf. Theory*, vol. 52, no. 4, pp. 1385–1398, Apr. 2006.
[16] V. Pauli, L. Lampe, and J. Huber, "Differential space–frequency modulation and fast 2-D multiple-symbol differential detection for MIMO-OFDM," *IEEE Trans. Veh. Technol.*, vol. 57, no. 1, pp. 297–310, Jan. 2008.
[17] D. Divsalar, S. Dolinar, and F. Pollara, "Serial concatenated trellis coded modulation with rate-1 inner code," in *Proc. IEEE GLOBECOM*, Dec. 2000, vol. 2, pp. 777–782.

[18] M. Tüchler, "Design of serially concatenated systems depending on the block length," *IEEE Trans. Commun.*, vol. 52, no. 2, pp. 209–218, Feb. 2004.
[19] L. Hanzo, O. Alamri, M. El-Hajjar, and N. Wu, *Near-Capacity Multi-Functional MIMO Systems (Sphere-Packing, Iterative Detection and Cooperation)*. New York, NY, USA: Wiley, 2009.
[20] S. Sugiura, "Dispersion matrix optimization for space–time shift keying," *IEEE Commun. Lett.*, vol. 15, no. 11, pp. 1152–1155, Nov. 2011.
[21] S. Sugiura, "Coherent versus non-coherent space–time shift keying for co-located and distributed MIMO systems," Ph.D. dissertation, Univ. Southampton, Southampton, U.K., 2010.
[22] M. Jiang and L. Hanzo, "Multiuser MIMO-OFDM for next-generation wireless systems," *Proc. IEEE*, vol. 95, no. 7, pp. 1430–1469, Jul. 2007.
[23] R. H. Clarke, "A statistical theory of mobile radio reception," *Bell Syst. Tech. J.*, vol. 47, no. 6, pp. 957–1000, Jul. 1968.
[24] V. Pauli and L. Lampe, "Tree-search multiple-symbol differential decoding for unitary space–time modulation," *IEEE Trans. Commun.*, vol. 55, no. 8, pp. 1567–1576, Aug. 2007.
[25] E. Chiavaccini and G. Vitetta, "Further results on differential space–time modulations," *IEEE Trans. Commun.*, vol. 51, no. 7, pp. 1093–1101, Jul. 2003.
[26] R. Schober and L. H.-J. Lampe, "Noncoherent receivers for differential space–time modulation," *IEEE Trans. Commun.*, vol. 50, no. 5, pp. 768–777, May 2002.
[27] B. L. Hughes, "Differential space–time modulation," *IEEE Trans. Inf. Theory*, vol. 46, no. 7, pp. 2567–2578, Nov. 2000.
[28] A. Burg, M. Borgmann, M. Wenk, M. Zellweger, W. Fichtner, and H. Bolcskei, "VLSI implementation of MIMO detection using the sphere decoding algorithm," *IEEE J. Solid-State Circuits*, vol. 40, no. 7, pp. 1566–1577, Jul. 2005.
[29] N. Seshadri and P. Hoeher, "On post-decision symbol-reliability generation," in *Proc. IEEE ICC*, May 1993, vol. 2, pp. 741–745.
[30] "Digital land mobile radio communications, final report," Office for Official Publications of the European Communities, Luxembourg, Tech. Rep., 1989.
[31] M. Patzold, *Mobile Fading Channels*. New York, NY, USA: Wiley, 2003.
[32] M. El-Hajjar and L. Hanzo, "EXITcharts for system design and analysis," *IEEE Commun. Surveys Tuts.*, vol. 16, no. 1, pp. 127–153, First Quarter 2014.
[33] J. Hagenauer, "The EXIT chart-Introduction to extrinsic information transfer in iterative processing," in *Proc. Eur. Signal Process. Conf.*, Vienna, Austria, Sep. 2004, pp. 1541–1548.

AUTHOR QUERY

NO QUERY.